Bulletin of the Seismological Society of America, Vol. 88, No. 1, pp. 43–61, February 1998

Bias in Surface-Wave Magnitude M_s due to Inadequate Distance Corrections

by Mehdi Rezapour and Robert G. Pearce

Abstract We investigate bias in surface-wave magnitude using the complete ISC and NEIC datasets from 1978 to 1993. We conclude that although there are some small differences between the ISC and NEIC magnitudes, there is no major difference between these agencies for this presentation of the global dataset. The frequency–distance plot for reported surface-wave amplitude observations exhibits detailed structure of the body-wave amplitude–distance curve at all distances; the influence of the surface-wave amplitude decay with distance is much less apparent. This censoring via the body waves represents a large deficit in the number of potentially usable surface-wave amplitude observations, particularly in the *P*-wave shadow zone between $\Delta = 100°$ and 120°. We have obtained two new modified M_s formulas based upon analysis of all ISC data between 1978 and 1993. In the first, the conventional logarithmic dependence of the distance correction is retained, and we obtain

$$M_s^e = \log(A/T)_{\max} + 1.155 \log(\Delta) + 4.269.$$

In the second, we make allowance for the theoretically known contribution of dispersion and geometrical spreading, to obtain

$$M_s^t = \log(A/T)_{\max} + \frac{1}{3}\log(\Delta) + \frac{1}{2}\log(\sin\Delta) + 0.0046\Delta + 5.370.$$

Comparison of these formulas with other work confirms the inadequacy of the distance-dependence term in the Gutenberg and Prague formulas, and we show that our first formula, as well as that of Herak and Herak, gives less bias at all epicentral distances to within the scatter of the observed dataset. Our second formula provides an improved overall distance correction, especially beyond $\Delta = 145°$. We show evidence that Airy-phase distance decay predominates at shorter distances ($\Delta \leqq 30°$), but for greater distances, we are unable to resolve whether this or non-Airy-phase decay predominates. Assuming 20-sec surface waves with $U = 3.6$ km/sec, we obtain a globally averaged apparent Q^{-1} of 0.00192 ± 0.00026 ($Q \approx 500$). We argue that our second formula not only improves the distance correction for surface-wave magnitudes but also promotes the analysis of unexplained amplitude anomalies by formally allowing for those contributions that are theoretically predictable. We conclude that there remains systematic bias in station magnitudes and that this includes the effects of source depth, different path contributions, and differences in seismometer response. For intermediate magnitudes, M_s^t shows less scatter against log M_0 than does M_s calculated using the Prague formula.

Introduction

Magnitude M is a measure of earthquake size determined from the amplitude and period of a certain type of seismic wave using an empirical formula that contains several constants whose values are chosen to maximize internal consistency between different observations. There is a limitation in the use of any magnitude scale for the quantification of earthquakes because magnitude is unrelated to source physics. Nevertheless, magnitude scales are so widely used that it is difficult to imagine that they would be easily abandoned. Moreover, archived magnitude data provide the only quantitative determinations of size for most historical earthquakes. Most studies in earthquake seismology use magni-

tude data as a guide to the strength of an earthquake. So biases in magnitude estimates, caused by incorrect allowance for any effects other than earthquake strength, directly affect the result of any study in which magnitude data are used. Such uses cover a wide range of seismology. Reduction of bias when comparing recent data (for which seismic moments can be determined) with historical data (for which only magnitudes are available) will improve estimates of the size of historical earthquakes, improve discrimination between earthquakes and nuclear explosions, and will give us a better measure of the overall rate of seismic energy release.

The problem of magnitude scale became very complex as many different scales were introduced to accommodate different situations such as the use of teleseismic surface and body waves, extension of the scale to intermediate and deep earthquakes, changes in seismic instrumentation, and extension of the scale to very small and very large earthquakes. Moreover, the standard magnitude estimates are meaningless for very large events (Aki, 1967; Kanamori, 1978) as the scale becomes saturated.

Earthquake magnitude is routinely estimated by the global agencies in two frequency bands: high-frequency body waves with periods around 1 sec (for m_b) and low-frequency surface waves with periods around 20 sec (for M_s). However, the period of the wave with maximum ground motion depends upon the source spectrum, the source depth, the dispersion characteristics and the absorption properties of the propagation path, and the magnification of the seismograph in the passband.

In this article, we consider bias in surface-wave magnitude M_s. There are two primary motivations. First, the M_s:m_b criterion is a widely used seismic discriminant between earthquakes and nuclear explosions, and it has potential to identify explosions under the Comprehensive Nuclear Test Ban Treaty. Second, the quantification of earthquake size requires a parameter that has a physical basis (e.g., seismic moment); such parameters for historical earthquakes must usually be derived from archived magnitude data. As the body of global magnitude data increases with the passage of time, there is more scope for understanding, and hence allowing for, its biases and scatter.

We begin by highlighting some theoretical points. We then compare m_b and M_s determinations for the two largest global agencies, the ISC (International Seismological Centre) and the NEIC (National Earthquake Information Center). We then examine M_s:m_b for the ISC data, and point out the large number of earthquakes that plot as explosions according to the M_s:m_b discriminant when ISC magnitudes are used. We then use the ISC global dataset to derive an optimum M_s distance-correction function, first assuming the "log(Δ)" distance dependence of conventional magnitude scales, and second after allowing for those parts of the distance dependence that are known from theory. These approaches are compared with each other and with other work. We also show the distribution of M_s against log M_0 for the Prague formula and for our second formula using 6553 earthquakes in the Harvard Centroid Moment Tensor (CMT) Catalogue. We then briefly consider the origins of the scatter remaining in M_s values.

Surface-Wave Magnitude Scales

Gutenberg Formula. Surface-wave magnitude was originally defined by Gutenberg (1945) as the first attempt to measure the strength of shallow earthquakes at teleseismic distances. As such, it was an extension of the local magnitude scale, M_L, introduced by Richter (1935) for the rating of regional earthquakes in California. The M_s scale was adjusted to agree with M_L and is based on 20-sec surface waves from shallow earthquakes in the distance range $15° \leqq \Delta \leqq 130°$. Richter introduced the universally accepted basis of magnitude as log (amplitude). However, there was no absolute scaling between the maximum amplitudes on instruments with different frequency responses, and the correction for distance was constrained to be logarithmic, without theoretical justification. Scales obtained from different instruments can be matched at one magnitude level, but they will then diverge at other levels (Scheidegger, 1985). The final formula of Gutenberg (1945) is

$$M_s^{\text{Gutenberg}} = \log A + 1.656 \log \Delta + 1.818 + S_c, \quad (1)$$

where S_c is a station correction, Δ is the epicentral distance in degrees, and A is the maximum amplitude on the horizontal component seismogram in microns for a surface wave with period of about 20 sec. This formula was originally designed to use amplitude data from horizontal seismographs, but when vertical-component systems came into general use, it became common practice to measure displacements on the vertical component.

Prague Formula. Vaněk *et al.* (1962) proposed the so-called "Prague formula":

$$M_s^{\text{Prague}} = \log (A/T)_{\max} + 1.66 \log \Delta + 3.3, \quad (2)$$

where A is the vertical or resultant horizontal amplitude in microns and T is the mean period in seconds. In equation (2), $(A/T)_{\max}$ is the maximum of all A/T (amplitude/period) values of wave groups on a record. However, it is not clear whether all the seismic stations that report data to the ISC measure $(A/T)_{\max}$ or $(A_{\max}/T)$. In practice, it seems improbable that $\log(A/T)_{\max}$ and $\log(A_{\max}/T)$ will differ greatly for classical long-period observations, though the difference may be very large on broadband seismograms, which are of course becoming more common. The Prague formula employed a geographic average of various distance-normalizing terms, and incorporated T in the formula to account for those cases, particularly for continental propagation and using broadband (Kirnos-type) seismographs, for which the

maximum trace amplitude does not occur at a period near 20 sec (Marshall and Basham, 1972).

The recommendations on magnitude made by the IASPEI (International Association of Seismology and Physics of the Earth's Interior) Assembly at Zürich in 1967 (Båth, 1981) concerned surface-wave magnitude determination using the Prague formula with conditions $20° \leqq \Delta \leqq 160°$, and 17 sec $\leqq T \leqq$ 23 sec for shallow earthquakes with a calculated depth $h < 50$ km. The ISC uses the Prague formula for shallow events with a calculated depth of $h \leqq 60$ km in the distance range 20° to 160° and in the period range 10 sec $\leqq T \leqq$ 60 sec. ISC uses either the vertical component or the vector sum of the horizontals, but NEIC uses only the vertical component.

Modified M_s Formulas. Several authors have pointed out difficulties with the above scales for $\Delta \leqq 20°$ (e.g., von Seggern, 1970; Evernden, 1971). A modification of the Prague formula applicable to closer ranges was proposed by Marshall and Basham (1972). They suggested a modified formula for M_s as

$$M_s = \log A_{\max} + B'(\Delta) + P(T) + 3, \qquad (3)$$

where A is the maximum amplitude in microns of the Rayleigh wave train, $B'(\Delta)$ is a tabulated epicentral distance correction term, and $P(T)$ is the path correction varying with the period of the wave measured and tabulated for different lithospheric structures. Marshall and Basham proposed that for distances up to 25°, the distance-dependence term, $B'(\Delta)$, is proportional to $0.8\log(\Delta)$, and at large teleseismic distances, it is the same as Gutenberg's distance-dependence term. Marshall and Basham have adjusted the absolute level of $B'(\Delta)$, so that magnitude determinations give results essentially the same as the Gutenberg and Prague formulas at large epicentral distances.

Herak and Herak (1993) found a new empirical formula for determining M_s as

$$M_s = \log (A/T) + 1.094 \log(\Delta) + 4.429 \qquad (4)$$

based on an analysis of surface-wave magnitudes of 250 selected earthquakes published in the ISC and NEIC Catalogues. They conclude that the Prague formula is inappropriate for magnitude determination because of bias in the distance calibration function.

The general form of most formulas for determining surface-wave magnitude has remained as

$$M_s = \log(A/T) + B(\Delta) + C,$$

where $B(\Delta)$ is a correction for the decay of amplitude with distance and C is a correction for effect of the station structure or path correction, which in some formulas has been omitted. Later we shall compute an M_s formula similar to equation (4), using a much larger dataset from the ISC.

Use of Theoretical Distance Corrections. The second and subsequent terms on the right of equations (1) to (4) attempt to correct individual observations for effects other than the earthquake strength, to ensure that the magnitude database is internally consistent and consistent with other magnitude scales. Okal (1989) considered the theoretical issues of magnitude corrections in some detail. He compared a theoretical distance correction with that of the Prague formula and found that the difference between these corrections never exceeds ± 0.05 magnitude units for $20° < \Delta < 150°$. Okal found that, compared with the theoretical distance correction, the Prague distance correction overestimates M_s by between 0.02 and 0.04 magnitude units in the distance range 20° to 110°. Nevertheless, he concluded that the distance correction of the Prague formula was adequate except at very short distances.

None of the above formulas incorporate corrections that are theoretically predicted, despite the fact that the main contributions to both distance and depth corrections are known from seismological theory, as pointed out by Nuttli (1973). Theoretically the distance-correction term is not logarithmic with distance, so there is a limit to the distance range over which the conventional correction can be applicable. This explains, at least in part, the difficulties with previous M_s distance-correction terms at short ($\Delta \leqq 20°$) and very long ($\Delta \geqq 140°$) distances. More importantly, in order to isolate those contributions to magnitude residuals that are unexplained, we must first correctly remove those components whose contribution is predictable from theory.

For a spherical Earth, and assuming that the wavelength is small compared with the Earth's radius, the distance dependence of Rayleigh-wave amplitude $A(\Delta,T)$ is given by (see, e.g., Marshall and Carpenter, 1966)

$$A(\Delta,T) \propto \Delta^{-\frac{1}{2}} (\sin \Delta)^{-\frac{1}{2}} \exp(-\pi^2 E\Delta/180QUT), \qquad (5)$$

where again Δ is the distance in degrees between source and receiver, U is the group velocity (which is assumed to be increasing monotonically with period T), E is the Earth's radius, and Q is the path-averaged apparent absorption coefficient for surface waves of period T. Here the three terms represent respectively the contributions of dispersion (Ewing *et al.*, 1957, p. 164), geometrical spreading on the surface of a sphere, and anelastic attenuation. For an observation at a known distance and period, this formula has only two unknowns—the product QU and the constant of proportionality. Near a group velocity minimum (corresponding to an Airy phase), the first term becomes $\Delta^{-1/3}$ (Ewing *et al.*, 1957, p. 165). Hence, the correction for dispersion depends upon whether or not the measured amplitude is at a period close to a group velocity minimum.

Thomas *et al.* (1978) examined the fit of a distance-correction function of this form and found that the Airy-phase dependence better fitted observations, which suggested that most of their observations were made from the

Airy phase. However, their data are restricted to stations of the Long Range Seismic Measurement (LRSM) program. Douglas *et al.* (1981) studied this in more detail and were unable to discriminate between non-Airy-phase decay and Airy-phase decay from the statistics of their regression lines.

Herak and Herak (1993) also considered a theoretical correction similar to equation (5), but they assumed non-Airy-phase observation in their dispersion term. Also, the formula they proposed did not include terms of a form corresponding to the theoretical corrections. Imposition of a distance dependence of the form of equation (5) does not increase the number of unknown constants to be determined by least-squares fitting of observations. Later we determine a distance correction function based on this form.

None of the commonly used surface-wave magnitude formulas include a depth-dependent correction, yet the effect of depth is known from theory to vary by about 1.0 magnitude units between 0 and 60 km for Love waves (e.g., Panza *et al.*, 1989); this corresponds to the range of computed values over which surface-wave magnitudes are determined by the ISC. It appears that failure to include such a correction results from the poor accuracy of depth determinations; it is not that the effect of depth is insignificant. Moreover, for earthquake/explosion discrimination, it is argued that the M_s:m_b criterion must work without a depth correction.

Comparison of Magnitudes Determined by ISC and NEIC

Magnitude is routinely estimated by different agencies, such as the ISC, NEIC, and by many national agencies, and at individual stations. For global comparison of magnitudes reported by the ISC and the NEIC, and for investigation of the M_s:m_b relation, we used the ISC Catalogue data from 1978 (when consistent ISC M_s determination began) to 1993. We use data from all earthquakes for which the ISC uses its own determination in the ISC Catalogue (i.e., where the ISC location is the "prime" location). The M_s:m_b statistics can be used for comparison of source properties only over a limited range of magnitudes since it is not linear over a large magnitude range. Figure 1 shows a comparison of magnitudes determined by the ISC and the NEIC in that period. Each graph includes those earthquakes (i.e., excluding events reported as explosions) for which the relevant two parameters are reported. ISC and NEIC compute M_s for earthquakes with a computed depth h of $\leqq 60$ km and < 50 km, respectively. To improve comparability, we impose a limit of $h < 50$ km for both agencies.

Many authors have given linear approximations to the relation between surface-wave and body-wave magnitudes. However, there is a great deal of scatter about the straight lines because of source effects and because of large variations, both random and systematic, in the empirical signals. These may be caused by differences in recording apparatus, the nonuniform distribution of seismic stations, and differences in the method of determination of magnitudes (Prozorov and Hudson, 1974). In Figures 1a and 1b, M_s versus m_b has been plotted for ISC and NEIC data, respectively. Regression lines have been determined assuming the same variance in M_s and m_b, and we obtain

$$M_s^{\mathrm{ISC}} = (1.8782 \pm 0.0222) m_b^{\mathrm{ISC}} - (4.6046 \pm 0.1102), \quad (6)$$

$$M_s^{\mathrm{NEIC}} = (1.8030 \pm 0.0216) m_b^{\mathrm{NEIC}} - (4.3655 \pm 0.1101). \quad (7)$$

Due to progressive increase in network sensitivity, the regression coefficient and regression constant in the linear regression line between M_s and m_b change significantly over time; we would expect this even if we imposed a magnitude cutoff and minimum number of reporting stations, because of the characteristic evolution of the global network. From the regression lines in Figures 1a and 1b, it is seen that in the ISC Catalogue, the values are equal at magnitude (M) about 5.2; for $M < 5.2$, surface-wave magnitude is less than body-wave magnitude, while for $M > 5.2$, the reverse is true. In the NEIC Catalogue, the values are equal at magnitude about 5.4. Correlation in Figure 1b (NEIC) is a little better than in Figure 1a (ISC).

In Figures 1c and 1d, a comparison is made between data for the two agencies, separately for body-wave and surface-wave magnitudes. The equations of the regression lines in Figures 1c and 1d are

$$m_b^{\mathrm{NEIC}} = (1.0053 \pm 0.0025) m_b^{\mathrm{ISC}} + (0.0166 \pm 0.0117), \quad (8)$$

$$M_s^{\mathrm{NEIC}} = (1.0089 \pm 0.0036) M_s^{\mathrm{ISC}} - (0.0743 \pm 0.0175). \quad (9)$$

In both Figures 1c and 1d, the correlation is good, but it seems that for body-wave magnitude, the correlation is higher for the NEIC than for the ISC. For surface-wave magnitude, the reverse is true. The correlation coefficient in equation (9) is higher than in equation (8). We conclude that although there are some small differences between the ISC and NEIC magnitudes, there is no major difference between these agencies for this presentation of the global earthquake data.

M_s:m_b for ISC Data

The relation M_s:m_b is widely used as a discriminant to identify underground nuclear explosions. The M_s:m_b discriminant is essentially empirical, with several effects contributing to its success. A number of studies have been carried out on the variation of M_s and m_b with geographical location. Marshall and Basham (1972) showed that the

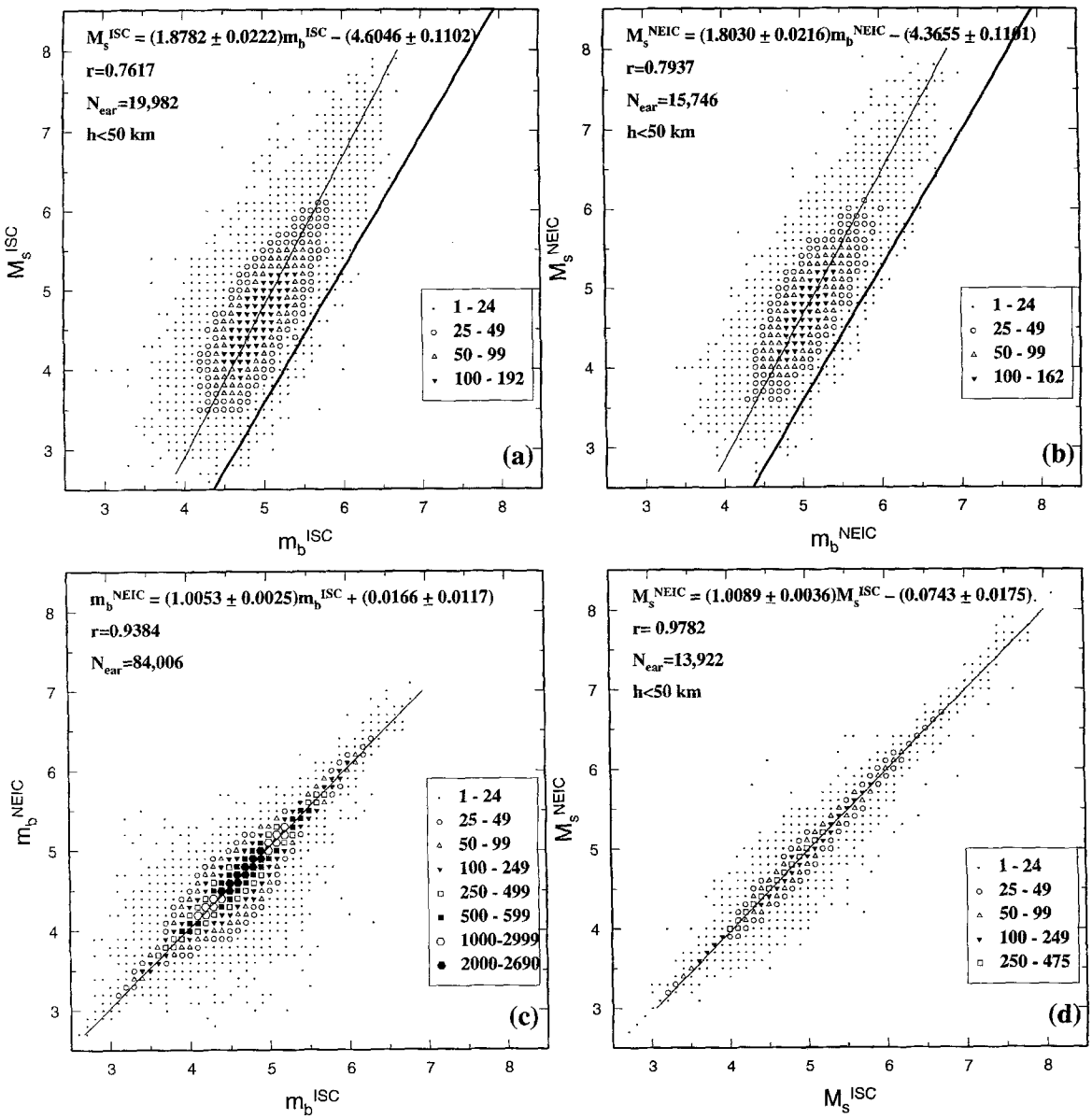

Figure 1. Relation between body-wave magnitude and surface-wave magnitude for earthquakes reported by ISC and NEIC from 1978 to 1993. (a) and (b) show surface-wave magnitude against body-wave magnitude. In (c), m_b^{ISC} versus m_b^{NEIC} and in (d), M_s^{ISC} versus M_s^{NEIC} is shown. Each plot includes all events for which the relevant two parameters have been reported, and the ISC is the "prime" location. In each case the regression line is shown by a thin solid line. r = correlation coefficient; N_{ear} = number of earthquakes; h = depth. Symbols indicate the number of data points as shown. In (a) and (b), the thick solid line shows the equation of $m_b = 0.595\ M_s + 2.872$ (Nowroozi, 1986), which is used as a discrimination line for earthquakes and underground nuclear explosions.

M_s:m_b relationship varies between different nuclear test sites. Although they found no such variation for earthquakes in the same regions, many workers have confirmed the geographical variation of M_s:m_b.

Examination from the viewpoint of the discrimination of earthquakes and explosions in the ISC and NEIC Catalogues shows that, respectively, about 2% and 2.84% of reported earthquakes used in Figures 1a and 1b are located to the right of the discrimination line formulated by Nowroozi (1986):

$$m_b = 0.595M_s + 2.872. \quad (10)$$

This line is marked in Figures 1a and 1b.

Figure 2a shows all the earthquakes that plot as explosions using ISC magnitudes. Because we are not comparing

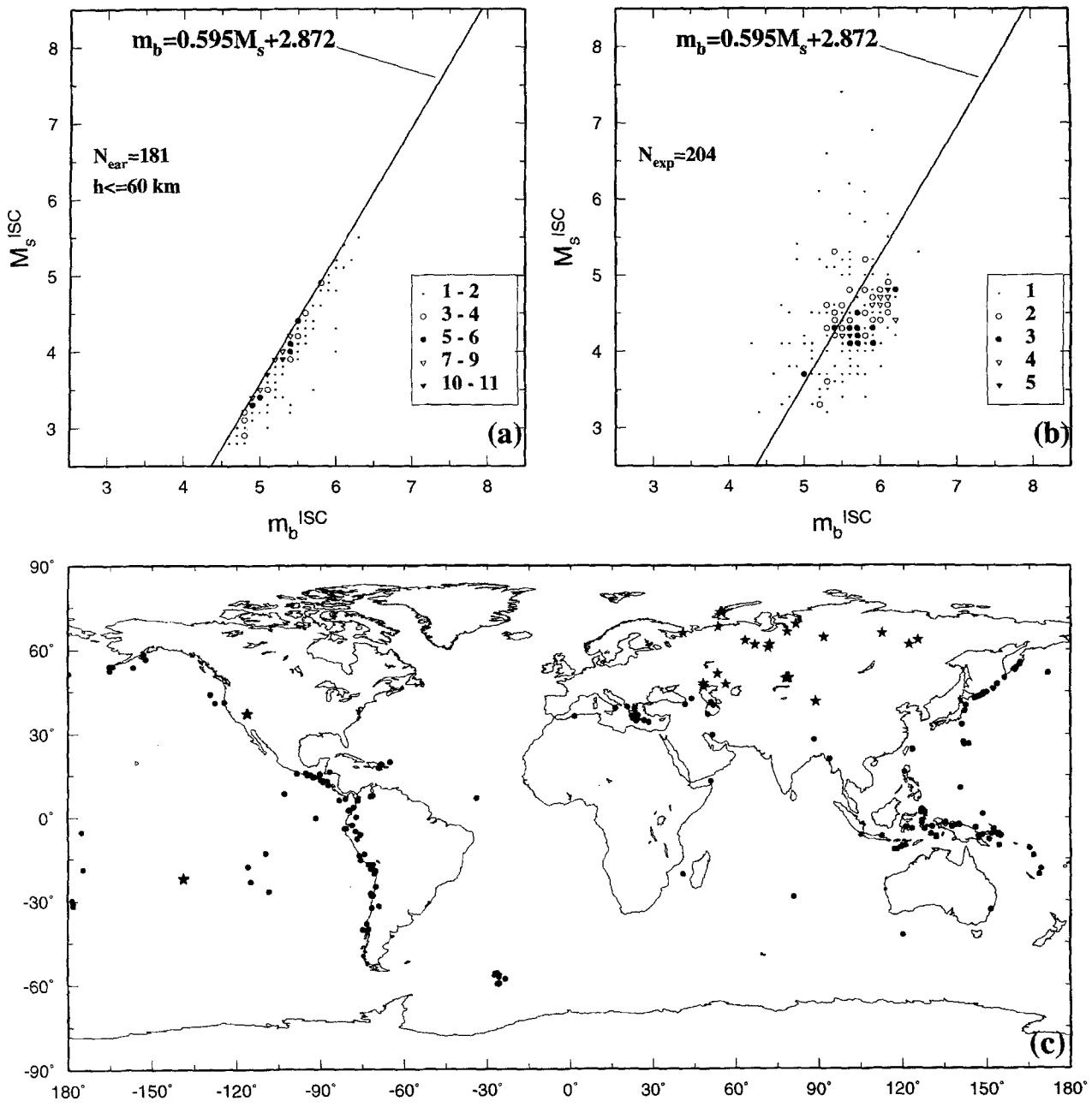

Figure 2. (a) Distribution of those events reported by the ISC as earthquakes that lie to the right of the discrimination line of Nowroozi (1986) in Figure 1a (including only earthquakes with a reported depth $h \leqq 60$ km); (b) Distribution all of events reported as underground nuclear explosions in the ISC Catalogue for which M_s is available; and (c) location of these earthquakes and explosions. In (a) and (b), symbols indicate the number of data points as shown; in (c), circles and asterisks denote the events in (a) and (b), respectively.

with NEIC data in this figure, we have included all earthquakes with a computed depth $h \leqq 60$ km. There are 181 earthquakes (0.82%) in Figure 2a out of a total of 22,080 ISC determinations with $h \leqq 60$ km. The worldwide distribution of these "anomalous" earthquakes is shown in Figure 2c; most are located in subduction zones. Figure 2b shows all events identified as nuclear explosions in the ISC Catalogue. For United States of America explosions, the "prime" determination is not that of the ISC, but these events have been included in the figure.

The question arises whether the absence of a depth correction in M_s is a major factor in these anomalous earthquake M_s:m_b ratios; this cannot be the case for the explosions because their depths are all close to zero. Because Figure 2a includes earthquakes with an ISC computed depth of $\leqq$60 km, the true depth of some of these events will be >60 km.

This implies failure to apply a depth correction to M_s for earthquakes with depths as great as (say) 80 km in some cases. Regression of M_s against depth for the anomalous earthquakes (without attention to errors in either parameter) gives a line of negative slope corresponding to an average M_s that is 0.2 units lower at $h = 60$ km than at zero depth. We expect the calculated M_s to be lower toward greater depth in the absence of a depth correction, but this result is only significant under the assumption that the true magnitude distribution is constant over this depth range. A histogram of these earthquakes against computed depth shows a steady increase in number with depth, whereas a histogram of all earthquakes for which M_s^{ISC} is available differ in that the number decreases for depths greater than 40 km. This shows that there are more anomalous earthquakes for depths at which the correction would be larger. We conclude that the absence of a depth correction is a contributory factor in these earthquakes, but the main factor appears to be nonsystematic.

The application of a depth correction to a given M_s value would always make events more earthquakelike, because observed surface-wave amplitude always decreases with true focal depth. However, as already pointed out, this would not assist discrimination by M_s:m_b; this must be achieved without a depth correction, because assignment of a nonzero depth itself implies prior identification of the source as an earthquake. Because explosions have a lower M_s:m_b ratio than earthquakes, the average distance of M_s observations will tend to be smaller for an explosion than for an earthquake with the same m_b. It follows that an inappropriate distance correction applied to surface-wave amplitudes will itself create bias in M_s:m_b ratios.

Kaverina *et al.* (1996) showed that the global distribution of "creepex" (difference between M_s and the orthogonal regression of M_s on m_b) has an evident pattern of dominance of negative values in subduction zones and positive ones in mid-ocean ridges. The name "creepex" was coined by combining two words: creep and explosion, which indicate the closeness of a seismic event by its spectral content either to ultra-low-frequency creep events or to high-frequency explosive ones (Kaverina *et al.*, 1996). A further clue to the problem of M_s:m_b using ISC data is given by Figure 2b, which shows all events reported as explosions by the ISC (and as such have a zero depth constraint).

Empirical Distance-Correction Function

To investigate the effect of distance on M_s determination, we determined station magnitudes (M_s^{STA}) from ISC Bulletin data using the Prague formula, for earthquakes with a published surface-wave magnitude (M_s^{ISC}) equal to 4, 4.5, 5, 5.5, 6, and 6.5 (M_s^{ISC} is essentially M_s averaged over contributing stations.) There are 851, 1383, 1039, 519, 229, and 82 earthquakes with estimated M_s of 4, 4.5, 5, 5.5, 6, and 6.5, respectively; and 89.5% of the measurements contributing to these data are from the vertical component. The difference ($M_s^{ISC} - M_s^{STA}$) is shown for these data in Figure 3. We do not attempt to reduce bias either by excluding poorly recorded earthquakes or by further limiting the distance range, because we wish to illuminate, rather than obscure, any factors that contribute to M_s values.

The differences in magnitude value established for

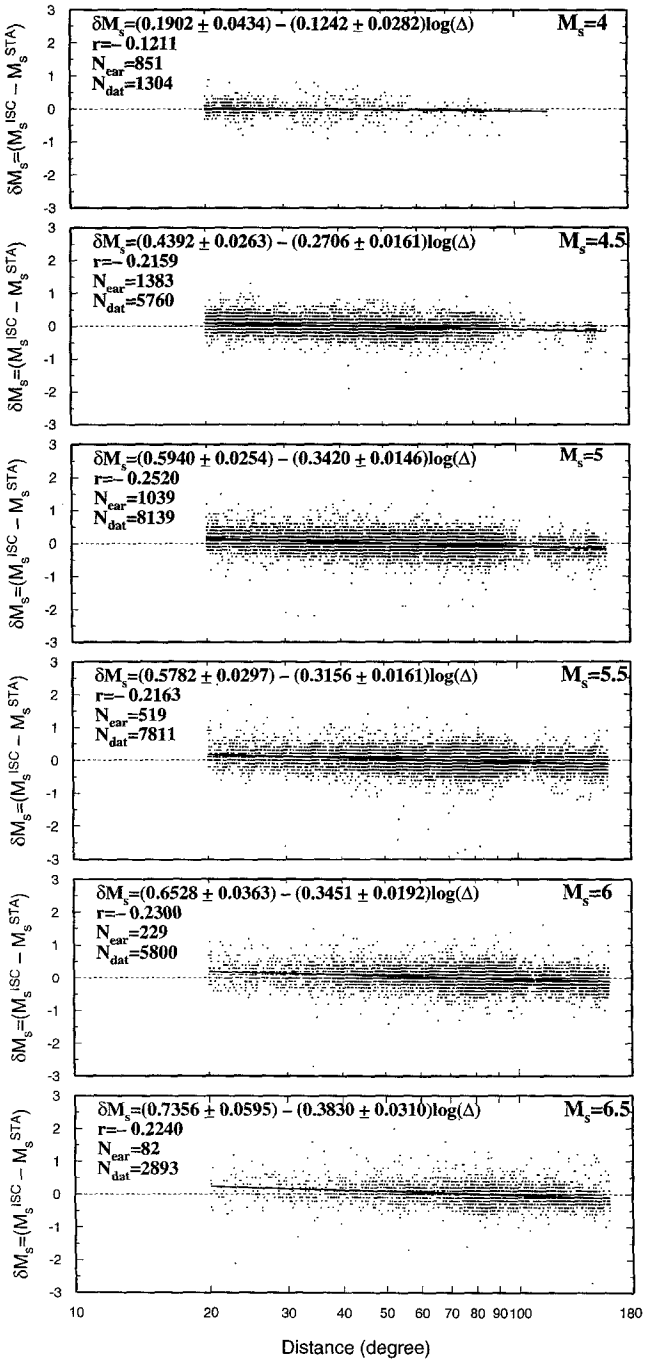

Figure 3. Deviation of individual station magnitudes from average magnitude, against distance for earthquakes with M_s^{ISC} equal to 4, 4.5, 5, 5.5, 6, and 6.5, which have been reported by the ISC from 1978 to 1993. N_{ear} = number of earthquakes; r = correlation coefficient; N_{dat} = number of station records.

waves of the same type at different stations are mainly due to different local conditions at the station, path effects, source effects, and instrumentation. In Figure 3, the slope of all regression lines is negative, which means that $M_s^{ISC} - M_s^{STA}$ decreases with increasing distance. In other words, M_s^{STA} for larger distances is overestimated, and for closer distances, is underestimated. Confirming the results of Herak and Herak (1993), this result indicates that M_s values obtained by the Prague formula are significantly distance dependent and that the numerical value of the constant 1.66 in the Prague formula is too large.

The regression lines in Figure 3 also show a systematic increase in negative slope with increasing magnitude. There are several possible reasons for this. First, the change in slope could arise from the different distribution of observations with distance at different magnitudes. If the distance term were correct, then all "ideal" M_s^{STA} values for earthquakes of the same magnitude would lie on a horizontal line, so that their mean (M_s^{ISC}) for any earthquake, and hence all values of $M_s^{ISC} - M_s^{STA}$, would be equal. Any error in the distance term (whether linear or nonlinear in log Δ) would cause M_s^{ISC} to depend on distance distribution, causing a scatter in values of $M_s^{ISC} - M_s^{STA}$. The systematic difference between station distance distributions at each magnitude would then cause a difference in the slope of the regression lines drawn through values of $M_s^{ISC} - M_s^{STA}$ at each magnitude. It follows that when the correct value of the constant in log Δ is applied, any nonlinear effect in log Δ can be revealed, and once an adequate correction is applied, any true dependence of the distance correction on magnitude can be isolated.

Second, M_s^{STA} values close to the maximum detection distance may be biased in favor of sensitive stations ($M_s^{ISC} - M_s^{STA}$ low), while for large earthquakes, the closest observations may be biased in favor of less-sensitive stations because of instrument saturation. These effects would cause similar slope changes as observed in Figure 3. We investigated this by replotting Figure 3, showing mean values of $M_s^{ISC} - M_s^{STA}$ for data binned in equal increments of distance. At each magnitude, we looked for curving downward or upward of those points near to the maximum and minimum of the distance range. There is some evidence of this at the upper distance limit for $M_s = 4$ and $M_s = 4.5$, and possibly at the lower end for $M_s = 6.5$. However, we conclude that the effect is unsufficient to contribute significantly to the changes in slope observed in Figure 3.

Third, it may be that the required distance-correction term is truly magnitude dependent, as a result of the magnitude dependence of source spectrum, the variation of different instrument response with period T, and a failure of the A/T term to compensate fully these effects when determining M_s^{STA}. We cannot distinguish between this and the first possibility until we have determined the optimum value for the log Δ correction.

In all the graphs of Figure 3, it is clear that, due to the P-wave shadow zone, the number of stations reporting to the ISC with epicentral distances between 100° and 120° is less than for other epicentral distances. The histogram of Figure 4 illustrates a limitation implicit in surface-wave observations in the ISC and most other agencies. Although the ISC will accept unassociated surface-wave observations, in practice, a surface wave is usually reported only if a direct P wave has already been identified. When the station is located in the shadow zone, the P-wave information is not usually reported; consequently, neither is the surface wave. (The distribution of body-wave observations is also shown in Fig. 4.) It follows that the form of the frequency–distance relation for single-station surface waves used in M_s determination is dominated by the structure of the body-wave amplitude–distance curve. The core shadow zone, PKP amplitude peak, and other features of the curve are closely reproduced, and this modulates the true surface-wave amplitude–distance effect, which tilts the distribution down toward increasing distance. A large proportion of data are located between Δ = 70° and 90°. This observed concentration is mainly due to the larger number of stations per unit distance at epicentral distances close to 90°, and to some extent on the nonrandom pattern of source–station distances over the Earth.

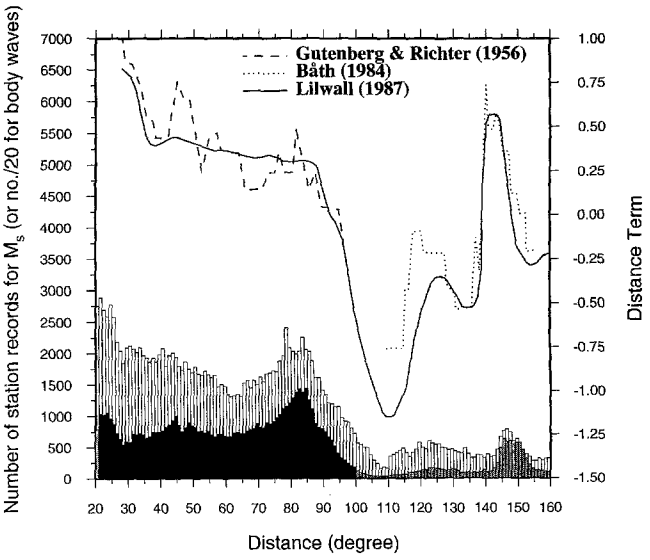

Figure 4. White histogram shows epicentral-distance distribution of 166,733 station records used in M_s^{ISC} determination for 22,080 earthquakes with ISC depth ≦ 60 km, between 1978 and 1993 (left scale). This is overlain by a histogram showing the epicentral-distance distribution of reported short-period P-wave amplitudes during the same period. This is shown in black for the range 21° ≦ Δ ≦ 100° that is used for m_b determination (1,268,101 station records for 110,300 earthquakes) and for other distances in gray (216,632 station records for 43,777 earthquakes). For this histogram, multiply the left scale by 20. The white and black histograms both exclude records outside the period limitation for the respective magnitude determination. Smoothed and unsmoothed published body-wave amplitude–distance curves are shown for comparison (right scale).

To re-examine the calibration function $B(\Delta)$, we used the method of Herak and Herak (1993), but for the whole ISC Catalogue data and using different conditions. In this study, we determined the parameters (α,β) of the regression line of station magnitude versus epicentral distance, for every earthquake with three or more stations in the computation of M_s^{ISC}.

To correct the calibration function $B(\Delta)$, we selected those data in the regression–coefficient range -2.5 to $+3.5$ with a standard error of fitting less than 0.5, and we plotted the difference between individual station magnitude and reference magnitude at $\Delta = 83°$ (M_{83}^j) versus the epicentral distance of the reporting station in Figure 5. As Figures 4 and 5 show, data are concentrated around $\Delta = 83°$, so the reference magnitude is defined as

$$M_{83}^j = \alpha^j + \beta^j \log(83°) \qquad (11)$$

for the jth earthquake ($j = 1 \ldots 9966$). The difference between individual station magnitude and relevant computed M_{83}^j is given by

$$\delta M_i(\Delta) = M_i^j(\Delta) - M_{83}^j, \qquad (12)$$

where i is the ith reported M_s for the jth earthquake ($j = 1 \ldots 9966$, $i = 1 \ldots N_j$). The results show that from 10,894 regression coefficients (β^j), only 2728 are negative, so that 75% of the data have a positive value. As Herak and Herak have pointed out, this indicates that M_s^{Prague} values are significantly distance dependent; consequently, the mean magnitude obtained by averaging all reported magnitude values is not a representative estimate of the earthquake's strength.

Equation (12) is plotted against epicentral distance for all data in Figure 5. The regression line is

$$\delta M_s = (0.5051 \pm 0.0037) \log \Delta - (0.9689 \pm 0.0066), \qquad (13)$$

so the modified Prague formula M_s^e (empirically corrected) becomes

$$M_s^e = \log(A/T)_{\max} + 1.555 \log \Delta + 4.269. \qquad (14)$$

Regression of mean observations binned in intervals of Δ had no significant effect on these regression parameters.

For $\Delta = 83°$, the Prague formula M_s (equation 2) and our M_s^e (equation 14) are equivalent, but for $\Delta = 20°$, equation (2) underestimates M_s by 0.31, whereas for $\Delta = 160°$, M_s is overestimated by 0.14 magnitude units. This result is not surprising; similar results have already been obtained by other workers such as von Seggern (1977), Thomas *et al.*, (1978), and Herak and Herak (1993). This study, which uses a much larger number of ISC data (from 1978 to 1993 over the full range of M_s^{ISC}), further emphasises the need to revise the Prague formula, which most agencies, including the ISC and NEIC, use to determine surface-wave magnitude. The value of the constant in equation (14) is dependent solely upon the choice of reference magnitude (or other condition imposed in the comparison of magnitude scales). It is now clear from Figure 5, as well as from theory, that the correction is not linear in log Δ.

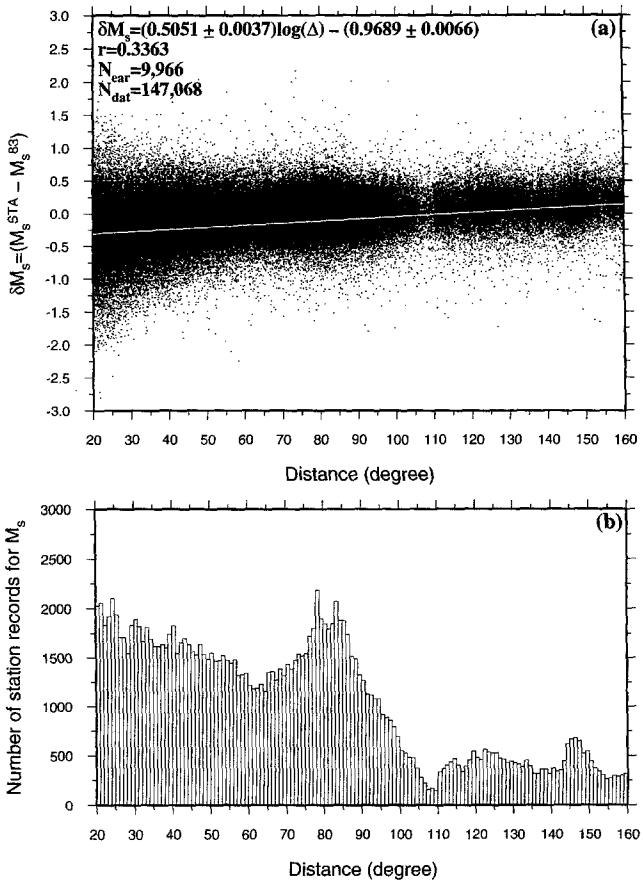

Figure 5. (a) Distribution of the differences between individual station magnitude and reference magnitude M_s^{83} against epicentral distance for 9966 earthquakes. The plot includes those earthquakes for which at least three observations have been used, and for which the regression line of station magnitudes against distance have a slope of between -2.5 and $+3.5$ and a standard error of less than 0.5. r = correlation coefficient; N_{ear} = number of earthquakes; N_{dat} = number of station records. The regression line (shown in white) is for δM_s against log Δ, although the graph is plotted linearly against Δ for clarity. (b) Histogram of distances of the constituent observations.

Empirical Distance Correction Function with Theoretical Constraints

In order to devise a magnitude M_s^t that incorporates theoretically predicted constraints in the distance-dependence terms in equation (5), we correct each A/T observation according to

$$(A/T)_{\text{corrected}} = (A/T)_{\text{observed}}(K\Delta^{-\alpha} \sin^{-\frac{1}{2}} \Delta e^{-k\Delta})^{-1}, \quad (15)$$

where α is either ½ (non-Airy-phase measurement) or ⅓ (Airy-phase measurement) and K and k are constants to be determined. The M_s^t definition becomes

$$M_s^t = \log(A/T) - \log K + \alpha \log \Delta + \frac{1}{2}\log(\sin \Delta) + k(\log_{10} e)\Delta. \quad (16)$$

Because the constant of proportionality in the log Δ term is not a free parameter, we still have only two constants to determine, as for previous formulas.

In order to estimate K and k, we choose the total distance-correction term for an individual observation as the difference between M_s^{ISC} for the corresponding earthquake and $\log(A/T)_{\text{station}}$ for the individual observation. We first use M_s^{ISC} because this is our best available estimate of M_s on the Prague scale. We set this distance correction to be the sum of the correction terms in equation (16), and rearranging, we obtain

$$M_s^{\text{ISC}} - \log(A/T)_{\text{station}} - \alpha \log \Delta - \frac{1}{2}\log(\sin \Delta) = k(\log_{10} e)\Delta - \log K. \quad (17)$$

This should correspond to a straight line of slope $k(\log_{10} e)$ and intercept $\log K$ if the left-hand side is plotted against Δ, and deviations from this straight line will represent additional effects not accounted for theoretically.

This procedure must be applied iteratively, replacing M_s^{ISC} by the average of the M_s^t values for each earthquake, $\overline{M_s^t}$, using equation (16) with K and k as determined. After three iterations, no further reduction was seen in the mean deviation of data from the regression line. The iteration procedure was repeated using $\overline{M_s^e}$ values for each earthquake as the initial values, computed using our equation (14). In this case, no iteration was required to reach minimum deviation. Figures 6a and 6b show this relationship for all station data (152,539 records from 10,894 earthquakes) with α = ⅓ and ½, respectively. The regression lines are shown in white, and the regression parameters are also shown. We see that there is an excellent linear trend over all distances. The fit is equally good in Figures 6a and 6b, so it appears that we cannot resolve from the observed data whether Airy-phase or non-Airy-phase measurements predominate. A similar conclusion was drawn by Douglas *et al.* (1981). Okal (1989) suggested that the assumption of Airy-phase observations made by some authors is probably invalid at periods close to 20 sec. In reality, the mixture of continental, oceanic, and mixed paths in global station magnitudes makes it difficult to make any prediction as to which, if either, type of observation will predominate over the period range of interest. However, our choice of α affects the value of k that is obtained, so the uncertainty in k must be increased to encompass values obtained with ⅓ ≦ α ≦ ½.

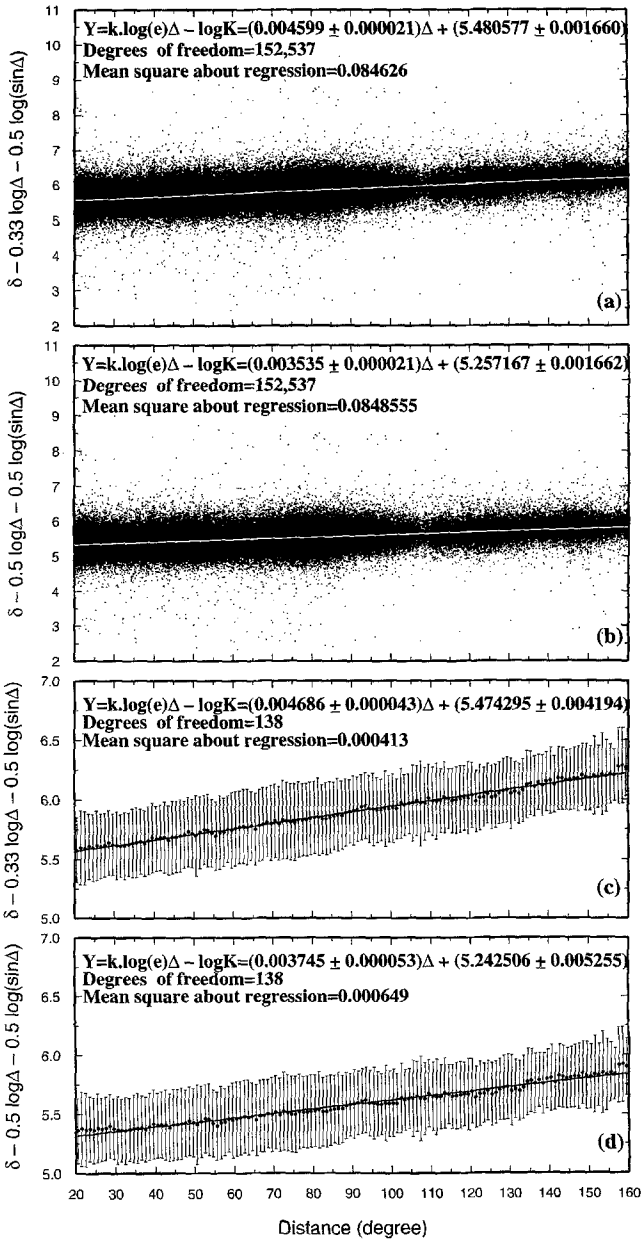

Figure 6. (a) The distance correction with the theoretically predicted parts removed assuming Airy-phase dispersion, plotted against epicentral distance. (b) as for (a) but assuming non-Airy-phase dispersion. (c) and (d), as for (a) and (b), respectively, but showing amplitude averaged in 1-deg bins with standard deviation. On all four graphs, $\delta = M_s^{\text{ISC}} - \log(A/T)_{\text{station}}$.

To examine the detail of the observed fit to the relationship represented in equation (17), we show in Figures 6c and 6d the mean of data in Figures 6a and 6b, respectively, binned for each 1° increment in Δ. Although the deviations are small compared with the standard error of each point, it is clear that adjacent values are not independent, so

that there are some details in the deviation that are systematic with distance. There is also a suggestion of an upward deviation for $\Delta < 30°$ in Figure 6d, which represents the only noticeable difference between Figures 6c and 6d. This suggests that at these close distances, Airy-phase measurements predominate (giving a straight line in Fig. 6c). We therefore chose $\alpha = \frac{1}{3}$, implying the overall predominance of observations close to an Airy phase. The random scatter in Figure 6a about the regression line is greater than ± 0.3 magnitude units. The absence of a depth correction should not directly affect the scatter in Figure 6 since these are differences between event-average and station measurements.

The value of K in equation (17) determines only the relationship between this and other scales, and it may be chosen to maximize consistency with them. The most compelling condition to impose would be equality at $\Delta = 20°$, to maintain consistency with M_L as originally intended by Gutenberg. However, this is unhelpful in practice because it would result in large corrections to the established scale over a large range of distances beyond 20° and, hence, a large correction to most existing magnitude determinations. An alternative condition is to leave the constant as it is; this corresponds to an agreement with the Prague formula at close to $\Delta = 83°$. Although this value was originally chosen because it represents the distance with greatest data density, a more appropriate condition for scale comparison is to set the constant so that the sum-squares correction needed to all ISC event magnitudes so far determined is minimized, i.e., we set K to $K - \delta$, where δ is chosen to minimize $\Sigma[M_s^{\mathrm{ISC}} - (\overline{M}_s^t + \delta)]^2$, where the sum is over all earthquakes. We find $\delta = 0.111$, so that the initial K value of 5.481 becomes $K = 5.370$. We then obtain the relation

$$M_s^t = \log(A/T)_{\max} + \frac{1}{3}\log(\Delta) + \frac{1}{2}\log(\sin\Delta) + 0.0046\Delta + 5.370. \quad (18)$$

According to the regression coefficient, i.e., $k \log_{10} e$ (see Fig. 6a), k is equal to 0.01050 ± 0.00005 deg^{-1}, and assuming 20-sec surface waves with group velocity of $U = 3.6$ km/sec, the globally averaged apparent Q^{-1} becomes 0.00218 ± 0.00001. Since we are unclear whether Airy-phase or non-Airy-phase measurements predominate (and, in general, we may expect a mixture), our best estimate and true error of Q^{-1} must include the uncertainty introduced by changing α from $\frac{1}{3}$ to $\frac{1}{2}$. We then obtain $Q^{-1} = 0.00192 \pm 0.00026$ ($Q \approx 500$), which is slightly higher than $Q = 405$ (with 95% confidence limits of 700 and 285) found by Marshall and Carpenter (1966) for the Northern Hemisphere. Von Seggern (1977) and Herak and Herak (1993) obtained somewhat higher values of $Q = 605 \pm 20$ and $Q = 704$, respectively, assuming $U = 3.5$ km/sec for 20-sec Rayleigh waves. The value of $Q = 297$ used by Okal (1989) is much lower because it was calculated assuming the Prague constant 1.66.

Comparison of Formulas

In Figures 7a and 7b, the distance calibration $B(\Delta)$ of different empirical formulas for determining M_s at 20-sec period are compared, and in Figure 7c, we show the differences between the distance corrections of our formulas and that of Prague. The differences in the slope of the calibration functions of Gutenberg, Prague, Herak and Herak, and our

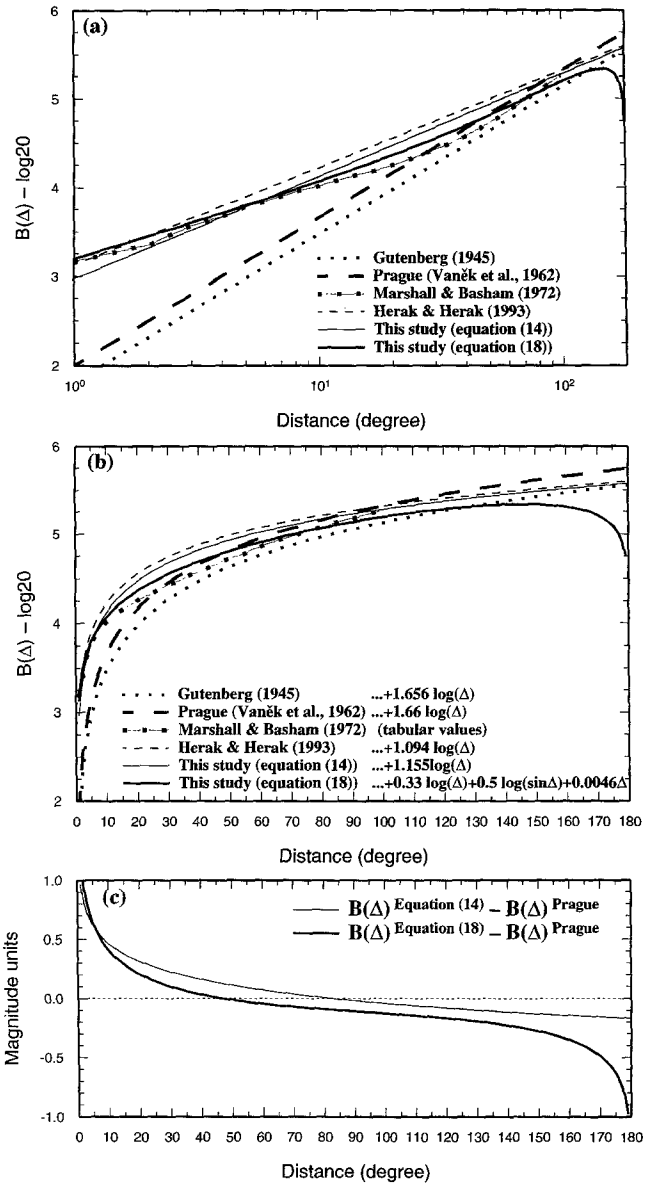

Figure 7. Distance-calibration functions $B(\Delta)$ for the determination of surface-wave magnitude using observations of 20-sec period for calibration functions of the following: Gutenberg without station correction, Prague, Marshall and Basham without path correction, Herak and Herak, our equation (14) (M_s^e), and our equation (18) (M_s^t). (a) On a log scale. (b) The same distance-calibration functions on a linear scale for more clarity. (c) Residual of our distance corrections for M_s^e and M_s^t compared with that of M_s^{Prague}.

M_s^e must be due to differences in the type of data used. For example, Gutenberg (1945) and Vaněk *et al.* (1962) used measurements made from horizontal components, whereas Herak and Herak (1993) used measurements of the vertical component. Here we use both types of measurement, of which only a small fraction of data (11.8% and 10.8% for the first and second formulas, respectively) were measured on horizontal components. Horizontal-component data may be either Love- or Rayleigh-wave amplitudes or a mixture of both. The specific quality factor for Love waves is less than for Rayleigh waves. So if most of the data are Love-wave amplitudes, a steeper slope is expected for the calibration function. Most importantly, we have used a distribution of data used by the ISC in its own magnitude determinations.

Comment is required on the vertical position of each curve in Figures 7a and 7b, which is governed solely by the constant term in the respective formula. We have pointed out that this depends only on the condition used to establish a comparison between the scales. The Prague formula is related to the Gutenberg formula by putting $T = 20$ sec, then using a different constant. The Marshall and Basham formula has the form 1.66 log Δ + constant for $\Delta > 40°$ and is approximately 0.8 log Δ + constant for $\Delta < 25°$. The Herak and Herak formula is set equal to the Prague formula at $\Delta = 100°$ by definition. Our first formula (M_s^e, equation 14) is equivalent to the Prague formula at $\Delta = 83°$ because of our different choice reference magnitude. Our second formula (M_s^t, equation 18) has been chosen to require minimum least-squares change in existing ISC magnitudes as explained in the previous section. (From Fig. 7, it is seen to equal M_s^{Prague} at $\Delta \approx 50°$ and to equal $M_s^{\text{Gutenberg}}$ at $\Delta \approx 130°$.)

To examine the accuracy of our formulas and other empirical formulas for the determination of M_s, 166,733 individual surface-wave magnitudes of 22,080 earthquakes recorded by 343 seismic stations were calculated. The deviation of individual station magnitudes from the average magnitude of the relevant earthquake computed using the same formula averaged in 1-deg-wide bins in distance, is shown in Figure 8. As observed in Figures 8c, 8d, and 8e, values of M_s determined by the Herak and Herak formula and our formulas are almost independent of distance within the range $20° \leqq \Delta \leqq 145°$. Our second formula (Fig. 8e) is independent of distance at least throughout the range $20° \leqq \Delta \leqq 160°$; this indicates an absence of distance bias when this formula is used.

By comparison with Figure 2a, the application of our M_s^t formula (equation 18) results in 149 earthquakes plotting in the explosion region, compared with 181 for the ISC Catalogue. For the explosion population, 63 explosions plot in the earthquake region, compared with 68 in Figure 2b. Because of our method of determining K, we expect the discrimination line of Nowroozi (1986) to behave similarly. We conclude that M_s^t:m_b may provide a small improvement in earthquake/explosion discrimination compared with M_s^{ISC}:m_b.

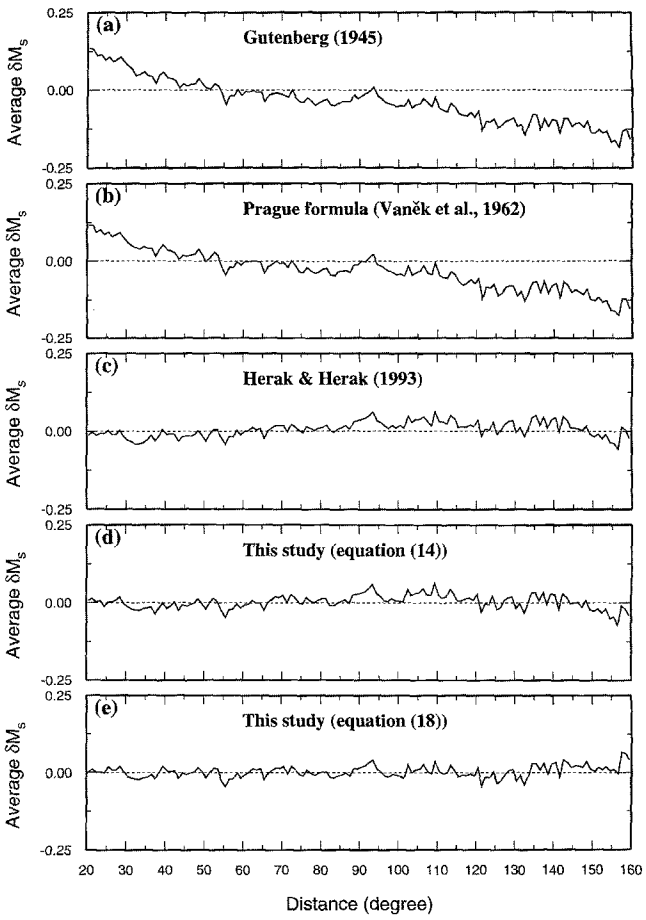

Figure 8. Observations of average magnitude residual for all earthquakes, binned at 1-deg distance intervals with individual magnitude calculated using (a) Gutenberg formula, (b) Prague formula, (c) Herak and Herak formula, (d) this study according to equation (14), and (e) this study according to equation (18). In all five cases, 166,733 station records were used from 22,080 earthquakes between 1978 and 1993. In all cases, the standard error of each point is approximately 0.25.

Relation between Seismic Moment M_0 and Magnitudes M_s^{Prague} and M_s^t

Ekström and Dziewonski (1988) studied bias in M_s by comparison with seismic moment M_0 and showed evidence of systematic deviations in M_s dependent upon tectonic setting. They concluded that M_s tends to overestimate the strength of most continental earthquakes and to underestimate it for those along mid-ocean ridges. They also concluded that estimates of seismic versus aseismic strain release may suffer because seismic moments determined from magnitudes can be wrong by as much as a factor of 4.

We now compare the relationship between seismic moment M_0 and two M_s scales, M_s^{Prague} and M_s^t (equation 18), using M_0 values obtained from the Harvard Centroid Moment Tensor (CMT) Catalogue that is available for a subset of earthquakes having body-wave magnitude of about 5 and

greater from 1977. In the CMT Catalogue, the prime location information is that of the NEIC PDE (*Preliminary Determination of Epicenters*), or in 23.5% of cases from its monthly listing. Where NEIC determinations are included in the ISC Catalogue, they are always from the monthly listing. We matched earthquakes by comparing the NEIC location in the ISC Catalogue to the CMT Catalogue, and imposing an origin time difference of $\leqq \pm 5$ sec and a latitude/longitude difference of $\leqq \pm 0.2°$. We matched 6553 earthquakes with a computed ISC depth $h \leqq 60$ km in this way, for the time period 1978 to 1993. This is of course a small number compared with the 22,080 we have used in previous sections.

To consider the difference in scatter of M_s about given values of M_0 when applying the Prague formula and our M_s^t, we plot in Figure 9 (a) mean $\overline{M_s^{\text{Prague}}}$ and (b) mean $\overline{M_s^t}$, against log M_0 binned in increments of 0.1 for these 6553 earthquakes from the CMT Catalogue. To show the range of M_0 values contributing to a given M_s value, Figures 9c and 9d present surface-wave magnitude binned against log M_0 using the same two M_s formulas, respectively. Here $\overline{M_s^{\text{Prague}}}$ and $\overline{M_s^t}$ are the magnitudes obtained for each earthquake to two decimal places using the contributing station amplitude and period values taken from ISC Bulletin data. Values of log M_0 are derived from M_0 values in the CMT Catalogue and are also expressed to two decimal places. ($\overline{M_s^{\text{Prague}}}$ differs from $\overline{M_s^{\text{ISC}}}$ only in some minor details of computation.)

Factors contributing to the relationship between M_s^{Prague} and M_0 observed in Figure 9a have been discussed by Hanks and Kanamori (1979) and by Ekström and Dziewonski (1988), whose analytical relationships are included as dashed and solid lines in Figure 9. Here we focus on the differences between the relationship observed using M_s^{Prague} and our M_s^t.

First, the differences between Figures 9c and 9d at the largest M_s values are not significant, as they result from small differences between M_s values for a small number of very large earthquakes. Second, from Figures 9a and 9b, M_s values are generally lower in 9b than 9a. This is because the figure includes only the larger earthquakes in the ISC Catalogue, whereas we have normalized our M_s^t scale to minimize differences over whole ISC dataset. Third, in 9b, the slope does not tend to 1.0 toward smaller magnitudes. Fourth, it is clear that the *b*-value obtained using the Prague formula on a large dataset will be different when we use instead our M_s^t (equation 18). Finally, there is significantly less scatter in log M_0 for a given M_s when M_s^t is used. This can be seen from Figures 9a′ to 9d′, which show differences between successive values in the histograms of 9a to 9d, respectively. This is particularly noticeable in the magnitude range 4.3 to 6.3 (compare Figs. 9c′ and 9d′).

Remaining Sources of Scatter and Bias in M_s

We now consider the scatter remaining in M_s^t values. We first reconsider the question posed by Figure 3, in which the distance dependence changed with magnitude. All the graphs in Figure 3 have been recomputed using our equation (18), so that the ordinate becomes $\overline{M_s^t} - M_s^t$. In all cases, the gradient of the regression line was $\leqq \pm 0.03$, with no systematic difference. We therefore conclude that there is no significant magnitude dependence in the distance-correction term of equation (18) over the whole distance range $20° \leqq \Delta \leqq 160°$.

Second, we re-examine the possible systematic effect arising from the absence of a depth correction to M_s. Romanelli and Panza (1995) conclude that this effect is significant. One way to examine it is to use CMT depth as a reference. Strictly, this approach is flawed in that centroid depth and depth of nucleation (deduced from travel-time data) are not coincident especially for large earthquakes. However, this difference will be insignificant compared with depth error for earthquakes below $M_s \approx 6.0$, because CMT depth is resolved to no better than 10 km, and the minimum error in ISC depth is similar. When the data in Figures 9c and 9d are plotted as separate curves for earthquakes with CMT depth in 20-km ranges, we see no significant difference between the curves for $0 \leqq h \leqq 20$ km and $20 < h \leqq 40$ km, but the curve for $40 < h \leqq 60$ km shows a systematic lower value of average M_s corresponding to 0.1 ± 0.05 magnitude units, throughout the magnitude range $4.7 \leqq M_s \leqq 6.3$. Above and below this range, the scatter increases, and any effect is obscured.

Third, the Prague formula has no station correction. Station correction may be influenced by seismograph type as well as local geological conditions. Historically, there has been a tendency for specific instrument types to be concentrated in specific regions—e.g., in the former Soviet Union; these regional differences are disappearing with the new generation of digital broadband instrumentation and the tendency toward more global mixing of seismograph types. It is therefore important to consider the extent to which regional differences in station magnitude residuals may be the result of regional clustering of common instrumentation.

From 1978 to 1993, the ISC has determined M_s for 22,080 earthquakes with $h \leqq 60$ km, using measurements from 343 seismic stations. There are 10,894 earthquakes for which three or more observations have been used in the calculation of M_s^{ISC}. For all 343 stations, the value of $\overline{M_s} - M_s^{\text{STA}}$ averaged over all earthquakes was computed using the Prague formula (M_s^{Prague}) and equation (18) (M_s^t). Values for those 231 seismic stations that have contributed M_s observations for more than 25 earthquakes are listed in Table 1. The absolute values of the average deviation for most (84%) of the stations is less than 0.2 magnitude units, but at some stations, this value is very high (see Table 1). Station BRS with the largest negative average ($\overline{\delta M_s}$) has been measured on vertical-component amplitudes, and for all its 52 readings, δM_s is negative. For station ALM where measurements have all been made on horizontal components, the reverse is true.

In Figure 10, the distribution of the deviation obtained

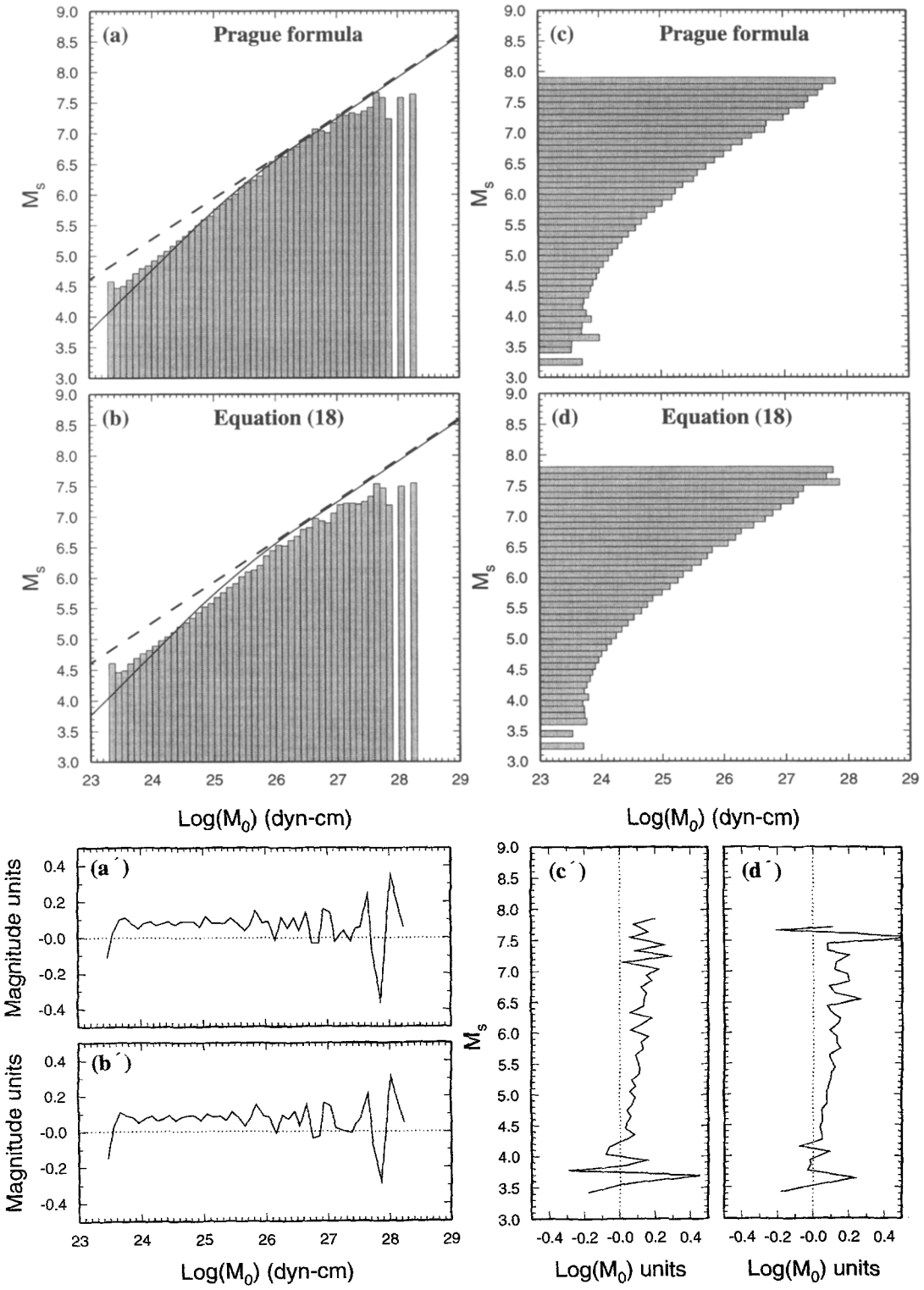

Figure 9. (a) Distribution of $\overline{M_s^{\text{Prague}}}$ averaged in 0.1-unit-wide ranges of log M_0 for 6553 earthquakes in the CMT Catalogue used in this study. (b) Shows the same using our $\overline{M_s^t}$ (equation 18). (c) and (d) Distribution of log M_0 for the same data, averaged in 0.1-unit-wide ranges of (c) $\overline{M_s^{\text{Prague}}}$ and (d) our $\overline{M_s^t}$. In (a) and (b), the dashed line shows the relationship obtained by Hanks and Kanamori (1979) under the assumption that the relationship is linear, and the solid line shows the analytical relationship developed by Ekström and Dziewonski (1988). (a′)–(d′) Difference between successive values in the histograms of (a)–(d), respectively.

Table 1

Mean Deviation $\overline{\delta M_s}$ of All Values of $\delta M_s = \overline{M_s} - M_s^{STA}$ for 231 Seismic Stations that ISC Has Used Measurements from for More Than 25 Earthquakes from 1978 to 1993

1*	2†	3‡	4§	1	2	3	4	1	2	3	4
AAA	−0.05 ± 0.20	−0.06 ± 0.20	42	HAU	0.11 ± 0.27	0.16 ± 0.26	1276	PPT	0.18 ± 0.56	0.08 ± 0.53	164
AAS	−0.20 ± 0.31	−0.26 ± 0.30	87	HFS	0.03 ± 0.31	0.07 ± 0.31	2677	PRA	−0.11 ± 0.26	−0.06 ± 0.23	750
ADK	0.12 ± 0.31	0.07 ± 0.27	49	HHC	−0.03 ± 0.20	−0.07 ± 0.20	2378	PRE	−0.11 ± 0.31	−0.07 ± 0.33	120
AKU	−0.05 ± 0.25	−0.05 ± 0.23	160	HLW	0.23 ± 0.42	0.22 ± 0.40	65	PRU	−0.11 ± 0.23	−0.06 ± 0.21	3684
ALM	1.10 ± 0.41	1.10 ± 0.42	35	HOF	−0.13 ± 0.23	−0.11 ± 0.21	229	PRZ	−0.17 ± 0.25	−0.20 ± 0.25	211
ALQ	0.01 ± 0.28	0.04 ± 0.28	3510	HON	0.17 ± 0.32	0.15 ± 0.30	893	PUL	−0.06 ± 0.26	−0.04 ± 0.25	536
ANMO	0.01 ± 0.31	0.03 ± 0.28	174	HRV	0.00 ± 0.25	0.04 ± 0.24	618	PYA	−0.11 ± 0.25	−0.08 ± 0.22	284
ANN	0.10 ± 0.21	0.12 ± 0.19	139	ILT	0.10 ± 0.33	0.08 ± 0.30	541	QIZ	0.09 ± 0.21	0.01 ± 0.21	583
ANR	−0.11 ± 0.27	−0.11 ± 0.25	378	IRK	0.05 ± 0.25	0.01 ± 0.25	1112	QZH	0.18 ± 0.21	0.10 ± 0.21	735
ANTO	0.18 ± 0.46	0.21 ± 0.47	35	ISA	0.01 ± 0.23	0.03 ± 0.23	448	RAC	−0.12 ± 0.28	−0.08 ± 0.28	213
APA	−0.13 ± 0.24	−0.11 ± 0.25	300	JCT	−0.04 ± 0.27	−0.02 ± 0.25	1219	RIV	0.38 ± 0.45	0.21 ± 0.47	95
APP	0.01 ± 0.30	0.07 ± 0.30	47	JFWS	−0.02 ± 0.23	0.00 ± 0.22	151	RJF	0.08 ± 0.30	0.14 ± 0.29	1100
ARC	0.10 ± 0.29	0.07 ± 0.29	46	KAT	−0.12 ± 0.34	−0.09 ± 0.32	242	RSCP	0.01 ± 0.36	0.01 ± 0.33	168
ARU	−0.12 ± 0.25	−0.10 ± 0.24	1082	KBS	−0.28 ± 0.84	−0.31 ± 0.81	58	RSNT	0.07 ± 0.24	0.05 ± 0.24	71
ASH	−0.15 ± 0.28	−0.15 ± 0.27	149	KEV	−0.07 ± 0.27	−0.06 ± 0.27	795	RSNY	0.04 ± 0.28	0.06 ± 0.28	908
ASPA	0.08 ± 0.35	0.00 ± 0.39	1672	KHC	−0.03 ± 0.27	0.02 ± 0.24	2335	RSON	0.03 ± 0.34	0.05 ± 0.33	369
BAK	−0.35 ± 0.38	−0.36 ± 0.36	103	KHE	−0.11 ± 0.29	−0.09 ± 0.28	432	RSSD	0.10 ± 0.31	0.12 ± 0.30	645
BCAO	0.10 ± 0.33	0.18 ± 0.31	76	KHO	0.05 ± 0.27	0.05 ± 0.26	54	SAM	−0.05 ± 0.27	−0.04 ± 0.26	259
BER	0.01 ± 0.71	0.02 ± 0.71	73	KIS	−0.10 ± 0.31	−0.05 ± 0.28	464	SAO	0.00 ± 0.27	0.00 ± 0.27	233
BINY	−0.07 ± 0.22	−0.01 ± 0.20	88	KIV	0.08 ± 0.27	0.14 ± 0.26	216	SBA	0.10 ± 0.26	0.04 ± 0.24	44
BJI	0.10 ± 0.23	0.07 ± 0.22	3402	KJF	−0.19 ± 0.22	−0.18 ± 0.22	867	SCO	−0.26 ± 0.41	−0.25 ± 0.39	46
BKR	−0.12 ± 0.31	−0.10 ± 0.30	42	KMI	−0.01 ± 0.25	−0.04 ± 0.24	1727	SDN	−0.01 ± 0.43	−0.02 ± 0.40	362
BKS	0.02 ± 0.33	−0.01 ± 0.33	1431	KOD	0.06 ± 0.22	0.00 ± 0.22	34	SEM	−0.08 ± 0.21	−0.08 ± 0.20	37
BLA	0.03 ± 0.29	−0.02 ± 0.28	211	KON	−0.24 ± 0.58	−0.26 ± 0.57	31	SEY	0.05 ± 0.31	0.00 ±0.26	199
BNS	−0.23 ± 0.29	−0.20 ± 0.27	360	KRA	−0.18 ± 0.26	−0.15 ± 0.24	2385	SHE	−0.05 ± 0.32	−0.04 ± 0.31	148
BOCO	0.17 ± 0.26	0.22 ± 0.25	40	KRV	0.14 ± 0.30	0.13 ± 0.29	82	SIM	0.03 ± 0.29	0.06 ± 0.27	355
BRG	−0.11 ± 0.22	−0.06 ± 0.21	1146	KSH	−0.26 ± 0.26	−0.25 ± 0.25	924	SIT	0.04 ± 0.35	0.03 ± 0.33	642
BRK	0.00 ± 0.31	−0.03 ± 0.30	151	KTG	−0.13 ± 0.26	−0.11 ± 0.27	77	SJG	0.06 ± 0.29	0.06 ± 0.27	433
BRS	−0.73 ± 0.29	−0.84 ± 0.33	52	KUL	−0.19 ± 0.26	−0.19 ± 0.27	49	SKO	−0.11 ± 0.38	−0.06 ± 0.37	1264
BRVK	0.00 ± 0.23	0.03 ± 0.22	72	KUR	0.10 ± 0.32	0.03 ± 0.29	262	SKR	0.18 ± 0.39	0.10 ± 0.37	84
BTO	−0.06 ± 0.21	−0.10 ± 0.21	2270	LBNH	−0.11 ± 0.21	−0.05 ± 0.22	102	SLL	−0.08 ± 0.37	−0.02 ± 0.36	102
BUL	−0.16 ± 0.33	−0.14 ± 0.34	230	LEN	0.21 ± 0.31	0.20 ± 0.29	59	SLM	0.02 ± 0.31	0.05 ± 0.30	367
CAR	0.05 ± 0.38	0.06 ± 0.39	182	LIC	0.11 ± 0.39	0.17 ± 0.38	700	SLR	−0.30 ± 0.36	−0.26 ± 0.35	1072
CBM	−0.05 ± 0.23	0.00 ± 0.21	348	LOR	0.06 ± 0.37	0.12 ± 0.36	1633	SMY	−0.01 ± 0.36	−0.05 ± 0.33	666
CCM	0.23 ± 0.33	0.25 ± 0.32	97	LPA	−0.02 ± 0.27	−0.02 ± 0.27	638	SNG	0.23 ± 0.40	0.10 ± 0.40	47
CD2	0.01 ± 0.21	−0.02 ± 0.21	1512	LPB	−0.10 ± 0.27	−0.07 ± 0.29	1647	SNY	0.02 ± 0.20	−0.02 ± 0.19	1792
CEH	0.08 ± 0.25	0.11 ± 0.24	565	LRG	0.05 ± 0.30	0.11 ± 0.29	491	SOC	−0.01 ± 0.30	0.01 ± 0.28	313
CHG	0.26 ± 0.38	0.22 ± 0.36	65	LSA	0.05 ± 0.30	0.01 ± 0.29	422	SPA	−0.03 ± 0.36	−0.05 ± 0.35	1757
CHTO	0.46 ± 0.49	0.45 ± 0.45	104	LSCT	−0.14 ± 0.21	−0.07 ± 0.22	86	SPC	−0.30 ± 0.39	−0.29 ± 0.38	122
CIT	−0.04 ± 0.27	−0.13 ± 0.28	126	LTX	0.05 ± 0.51	0.07 ± 0.50	193	SRO	−0.14 ± 0.31	−0.12 ± 0.30	563
CLL	−0.02 ± 0.22	0.02 ± 0.20	926	LVV	−0.20 ± 0.31	−0.16 ± 0.29	306	SSE	0.12 ± 0.26	0.07 ± 0.25	3226
CMB	0.04 ± 0.25	0.05 ± 0.25	425	LZH	−0.02 ± 0.24	−0.04 ± 0.24	3873	SSPA	0.21 ± 0.48	0.25 ± 0.47	35
CN2	0.01 ± 0.23	−0.01 ± 0.22	2292	MAK	−0.04 ± 0.32	−0.04 ± 0.30	248	STAN	0.10 ± 0.25	0.05 ± 0.25	34
COL	0.00 ± 0.29	−0.02 ± 0.27	668	MAT	0.22 ± 0.27	0.17 ± 0.25	2741	STU	0.04 ± 0.24	0.06 ± 0.22	269
COP	−0.06 ± 0.27	−0.03 ± 0.26	776	MAW	−0.08 ± 0.33	−0.10 ± 0.35	263	SUR	−0.32 ± 0.32	−0.31 ± 0.31	232
CTA	−0.02 ± 0.37	−0.17 ± 0.37	280	MCWV	−0.10 ± 0.27	−0.07 ± 0.24	333	SVE	−0.10 ± 0.29	−0.08 ± 0.29	974
CTAO	0.15 ± 0.43	0.07 ± 0.44	26	MDJ	0.01 ± 0.23	−0.03 ± 0.23	1053	TAS	−0.08 ± 0.27	−0.07 ± 0.26	523
DAG	−0.05 ± 0.30	−0.04 ± 0.30	308	MGD	0.17 ± 0.34	0.13 ± 0.29	472	TIA	0.07 ± 0.21	0.02 ± 0.21	1514
DBN	0.09 ± 0.29	0.11 ± 0.28	1133	MHC	0.09 ± 0.44	0.06 ± 0.42	163	TIK	−0.02 ± 0.27	−0.03 ± 0.26	842
DL2	0.16 ± 0.27	0.11 ± 0.26	976	MIAR	0.13 ± 0.25	0.17 ± 0.22	362	TIY	−0.08 ± 0.22	−0.09 ± 0.20	2963
DOU	−0.04 ± 0.22	−0.01 ± 0.21	458	MIN	0.16 ± 0.51	0.13 ± 0.52	40	TLG	0.12 ± 0.31	0.10 ± 0.31	331
DSH	−0.05 ± 0.29	−0.05 ± 0.29	62	MIR	0.04 ± 0.26	0.00 ± 0.28	133	TPNV	−0.18 ± 0.30	−0.18 ± 0.29	191
DUG	0.10 ± 0.23	0.13 ± 0.23	230	MNK	−0.24 ± 0.22	−0.20 ± 0.20	179	TUC	0.06 ± 0.26	0.08 ± 0.26	404
ELT	−0.15 ± 0.31	−0.16 ± 0.31	254	MOS	−0.17 ± 0.28	−0.16 ± 0.26	512	TUL	0.09 ± 0.37	0.11 ± 0.35	2828
ERE	0.11 ± 0.28	0.12 ± 0.28	96	MOX	−0.04 ± 0.24	0.00 ± 0.24	2764	UER	0.02 ± 0.33	−0.03 ± 0.34	72
FLN	0.05 ± 0.28	0.10 ± 0.28	1089	MSO	0.00 ± 0.48	0.00 ± 0.48	119	UKR	0.02 ± 0.20	−0.01 ± 0.18	29
FRU	−0.06 ± 0.24	−0.06 ± 0.23	677	MTA	0.32 ± 0.36	0.35 ± 0.36	140	UPA	0.12 ± 0.32	0.13 ± 0.29	496
FUR	−0.06 ± 0.29	−0.03 ± 0.28	582	MUN	−0.01 ± 0.32	−0.12 ± 0.34	363	UZH	−0.21 ± 0.30	−0.16 ± 0.27	435
FVM	−0.14 ± 0.33	−0.11 ± 0.30	479	NAI	0.23 ± 0.37	0.25 ± 0.37	180	VKA	0.07 ± 0.22	0.10 ± 0.21	713
GAC	−0.15 ± 0.75	−0.16 ± 0.76	27	NDI	0.11 ± 0.33	0.07 ± 0.32	373	VLA	0.37 ± 0.47	0.29 ± 0.46	77

(*continued*)

Table 1—*Continued*

1*	2†	3‡	4§	1	2	3	4	1	2	3	4
GAM	−0.43 ± 0.99	−0.45 ± 1.01	28	NEW	−0.11 ± 0.35	−0.11 ± 0.34	663	WAR	−0.23 ± 0.24	−0.21 ± 0.23	447
GAR	0.06 ± 0.37	0.05 ± 0.36	56	NJ2	0.16 ± 0.25	0.11 ± 0.24	1332	WDC	0.05 ± 0.28	0.07 ± 0.28	402
GDH	−0.04 ± 0.25	−0.03 ± 0.25	269	NNA	0.26 ± 0.42	0.26 ± 0.42	419	WEL	−0.09 ± 0.29	−0.21 ± 0.27	170
GLD	−0.04 ± 0.31	−0.03 ± 0.29	1249	NRI	−0.21 ± 0.31	−0.22 ± 0.29	505	WET	−0.12 ± 0.24	−0.09 ± 0.22	337
GOGA	0.04 ± 0.22	0.08 ± 0.20	81	NRN	−0.29 ± 0.36	−0.31 ± 0.36	36	WHN	0.04 ± 0.22	−0.01 ± 0.22	1554
GOL	0.06 ± 0.28	0.08 ± 0.27	1817	NUR	−0.03 ± 0.27	0.00 ± 0.27	2696	WIN	−0.29 ± 0.34	−0.26 ± 0.34	367
GRA1	−0.09 ± 0.63	−0.08 ± 0.62	26	NVL	−0.06 ± 0.30	−0.06 ± 0.30	360	WMOK	−0.05 ± 0.24	−0.01 ± 0.22	251
GRB1	0.10 ± 0.51	0.14 ± 0.50	70	NVS	−0.14 ± 0.26	−0.16 ± 0.26	357	WMQ	−0.12 ± 0.24	−0.10 ± 0.23	2684
GRF	0.10 ± 0.28	0.15 ± 0.27	3938	NWAO	0.22 ± 0.38	0.17 ± 0.40	629	WOL	−0.10 ± 0.83	−0.05 ± 0.82	81
GRM	0.02 ± 0.40	0.04 ± 0.40	179	OBN	−0.13 ± 0.26	−0.08 ± 0.25	1695	XAN	−0.02 ± 0.23	−0.05 ± 0.22	1358
GRO	−0.28 ± 0.32	−0.26 ± 0.33	306	OJC	−0.12 ± 0.30	−0.07 ± 0.28	105	YAK	0.05 ± 0.26	0.00 ± 0.24	595
GRS	0.16 ± 0.29	0.17 ± 0.28	272	ORV	0.19 ± 0.25	0.19 ± 0.24	53	YBH	0.09 ± 0.21	0.08 ± 0.22	50
GTA	−0.12 ± 0.22	−0.12 ± 0.22	3216	PAS	0.12 ± 0.27	0.10 ± 0.25	300	YSNY	−0.06 ± 0.22	−0.01 ± 0.21	101
GUA	0.32 ± 0.27	0.17 ± 0.28	457	PET	0.19 ± 0.29	0.14 ± 0.25	431	YSS	0.16 ± 0.29	0.12 ± 0.26	721
GUMO	0.48 ± 0.34	0.39 ± 0.34	526	PME	0.07 ± 0.40	0.04 ± 0.38	201	ZAK	−0.04 ± 0.23	−0.08 ± 0.23	1188
GYA	0.02 ± 0.21	−0.02 ± 0.22	1599	PMG	0.02 ± 0.40	−0.08 ± 0.41	127	ZOBO	0.12 ± 0.28	0.20 ± 0.29	1475
GZH	0.09 ± 0.22	0.02 ± 0.23	756	PMR	0.10 ± 0.32	0.10 ± 0.30	1849	ZST	−0.27 ± 0.40	−0.23 ± 0.39	173

*Station code.
†Mean deviation with standard error ($\overline{\delta M_s} \pm \sigma_{\text{mean}}$) according to the Prague formula.
‡Mean deviation with standard error ($\overline{\delta M_s} \pm \sigma_{\text{mean}}$) according to equation (18).
§Number of readings.

using the Prague formula for these stations has been plotted on a world map. Stations located in southern Africa, the eastern part of Europe, and in the former Soviet Union have negative deviations. This means that the sizes of events have been overestimated relative to other seismic stations, and for some other stations, the reverse is true. Therefore, corrections are essential to improve the measure of earthquake size obtained from M_s. This is not unexpected, and station magnitude residuals have long been used as an indicator of regional seismic attenuation. However, we would like to differentiate between true near-station effects caused by subsurface conditions, and any purely instrumental effect that may result from biases due to the prevalence of different recording instruments in different regions of the world. Unfortunately, comprehensive information on the type of instrument used is not easily available for most stations. From future studies using exclusively digital data transformed to a common instrument response, it will be possible to isolate any contribution of instrumentation, from which we will be able to decide whether an investigation into this aspect of previous data would be worthwhile.

Fourth, the Prague formula has no path correction, although the substantial effect on M_s^{STA} of surface-wave propagation path has long been well known. From our equation (18), it follows that the appropriate way to introduce a path correction into our M_s^t scale would be to determine a path-specific value of K, since this constant reflects both the average anelastic attenuation along the path and the average velocity structure. This implies that the path correction would be linear in distance Δ.

Fifth, we know that azimuthal variation in surface-wave radiation pattern must contribute significantly to scatter in M_s^{STA}. It has long been recognized that station M_s determinations must not require prior focal mechanism determination and that source radiation effects are expected to remain as a contributory factor in M_s scatter.

Finally, there is a scatter implicit in the observatory practice of measuring surface-wave amplitude. Figure 11 shows the distribution of amplitude and period values among observations. Similar to the data of Douglas *et al.* (1981), we see a predominance of "round number" values in A and T for the ISC data, which is evident from the peaks at multiples of 0.1 μm and 2 sec in amplitude and period, respectively, in Figure 11a. This is made clear in the magnified section of 11a, shown in 11b. It is known that the most important source of this type of effect is associated with recording system. In particular, many WWSSN stations recorded at 0.5 mm/sec, while many observers read times to the nearest millimeter. This measurement practice results in various preferred $\log(A/T)$ values. The effect of this on larger-magnitude values is insignificant, but the effect becomes progressively larger toward smaller magnitudes. For example, it seems the precision of most amplitude measurements is ± 0.05 μm. For a measured value of 0.1 μm ($M_s \approx 4$), this implies an error of ± 0.18 magnitude units, whereas at 0.01 μm ($M_s \approx 3$), this gives an error of ± 0.8 magnitude units.

Conclusions

A global comparison of magnitude determinations by the ISC and NEIC shows some small differences, but there are no systematic differences between reported magnitudes of ISC and NEIC. A least-squares fit of 19,982 M_s and m_b values reported by the ISC for the period 1978 to 1993 gives

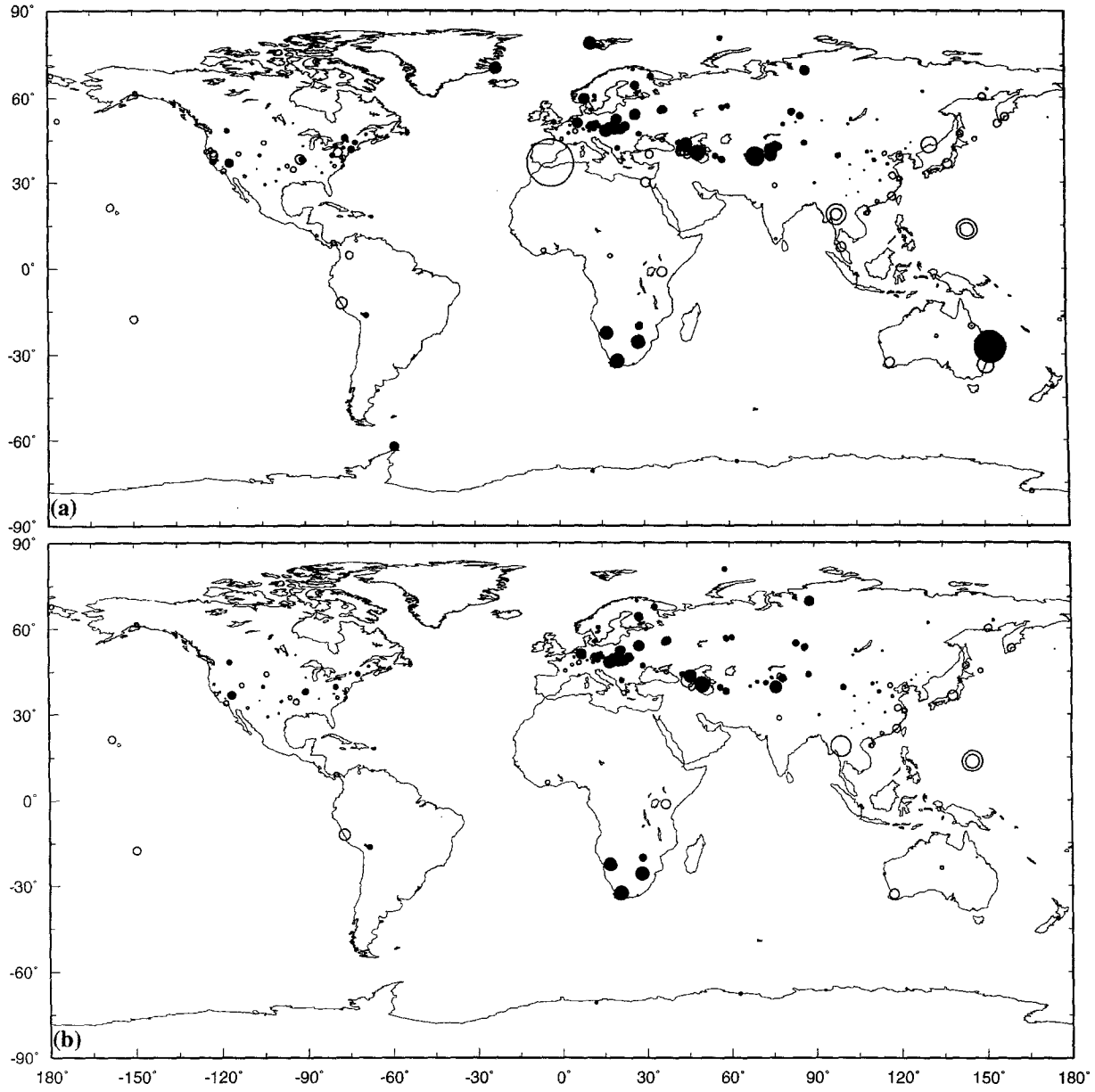

Figure 10. Global maps showing the average value of $\overline{M_s} - M_s^{STA}$ for all earthquakes recorded at individual stations. (a) Includes those stations that have contributed more than 25 earthquakes. (b) Stations that have contributed more than 100 earthquakes. Filled circles show positive deviations ($\overline{M_s} > M_s^{STA}$), and open circles show negative deviations. The size of each circle is proportional to the absolute value of the mean deviation; the largest symbol corresponds to a deviation of 1.12 magnitude units.

$$M_s^{ISC} = (1.8782 \pm 0.0222)m_b^{ISC} - (4.6046 \pm 0.1102),$$

and the relation of M_s and m_b values of 15,746 earthquakes reported by the NEIC in that period is

$$M_s^{NEIC} = (1.8030 \pm 0.0216)m_b^{NEIC} - (4.3655 \pm 0.1101).$$

The number of reported surface-wave amplitude observations at distances corresponding to the *P*-wave shadow zone ($100° \leqq 120°$) is less, because most seismic stations measure surface waves after recognizing the first-arrival *P* wave. Indeed, the frequency–distance relation for surface-wave amplitude measurements is dominated by the body wave amplitude–distance curve. It follows that many potentially useful observations of surface-wave amplitude are missing from the datasets.

In an investigation of the distance calibration function, we conclude that in the Herak and Herak formula and our

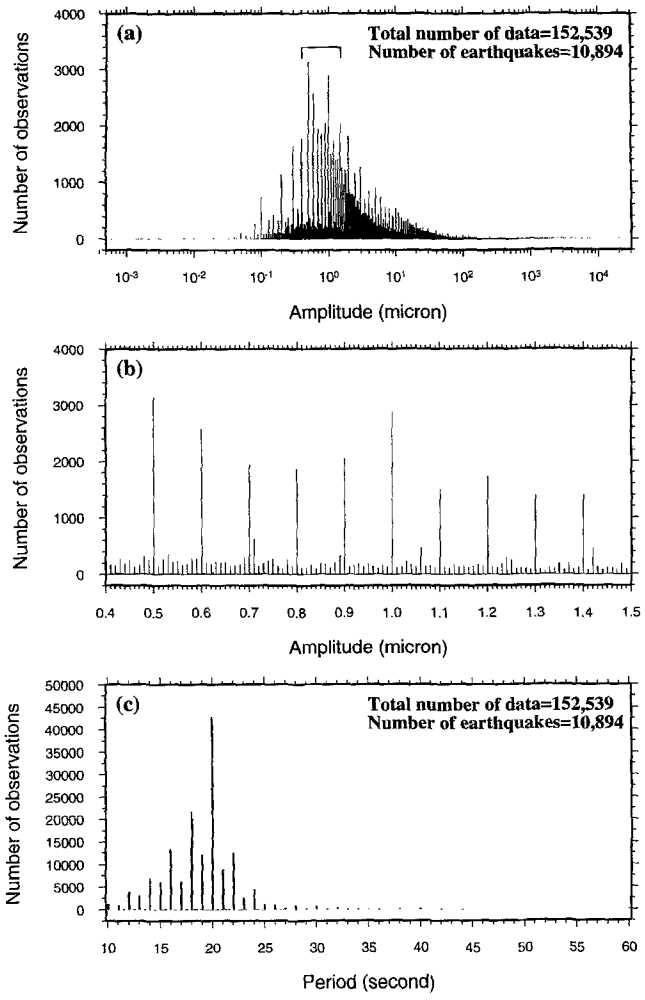

Figure 11. Histograms of measured amplitude and period of surface waves for all observations of earthquakes for which three or more reported observations have been used in the calculation of M_s^{ISC}: (a) for amplitude (in microns) on logarithmic scale, (b) for a small part of the amplitude range identified in Figure 11a plotted on a linear scale for more clarity, and (c) for period in seconds.

M_s^e and M_s^t formulas, the residuals of individual station magnitudes from the mean magnitudes are less than for other formulas. Our M_s^e (equation 14) was obtained using the whole ISC data from 1978 to 1993 and over the whole range of M_s. By deriving a formula containing theoretical distance-dependence terms, we have provided a means (M_s^t, equation 18) to reduce systematic errors in the distance correction over the full range of distances. There is some evidence that Airy-phase, rather than non-Airy-phase, distance dependence dominates measurements for $\Delta < 35°$.

Deviations in M_s determinations made using our M_s^t formula isolate those remaining sources of scatter that are unexplained. It appears that the absence of a depth correction and of station and path corrections all contribute to this remaining scatter but that there is no discernible magnitude dependence remaining in our M_s^t distance correction. It is possible that regional variations in instrumentation are distorting the perceived regional differences in M_s station residuals, but further investigation of this must await more seismic moment data from the global digital networks. We have shown that there is less scatter in the relationship between our M_s^t and CMT M_0 than when M_s^{Prague} is used.

The kind of study reported here is important in the removal of bias in M_s. It is also important in the correct application of the M_s:m_b discriminant, and in confirming the need to modify the formula for M_s calculation. In particular, we have shown the importance of applying a suitable distance-correction term that is theoretically valid.

Acknowledgments

We thank Professor A. Douglas and Drs. D. Bowers and D. McCormack for their valuable comments. We also thank associate editor Dr. Lind Gee, reviewer Dr. Göran Ekström, and one anonymous reviewer, for suggesting improvements to the original manuscript. One of us (M.R.) was supported by a scholarship from the Ministry of Culture and Higher Education of Iran. The figures were prepared using Generic Mapping Tools (Wessel and Smith, 1995).

References

Aki, K. (1967). Scaling law of seismic spectrum, *J. Geophys. Res.* **72,** 1217–1231.

Båth, M. (1981). Earthquake magnitude—recent research and current trends, *Earthquake Sci. Rev.* **17,** 315–398.

Båth, M. (1984). Earthquake magnitude based on *PKP* and *SKP* waves, *Boll. Geofis. Teor. Appl.* **26,** 93–108.

Douglas, A., J. B. Young, and P. D. Marshall (1981). Some analyses of *P*- and Rayleigh-wave amplitudes observed at North America stations, *Geophys. J. R. Astr. Soc.*, **67,** 305–324.

Ekström, G. and A. M. Dziewonski (1988). Evidence of bias in estimations of earthquake size, *Nature* **332,** 319–323.

Evernden, J. F. (1971). Variation of Rayleigh-wave amplitude with distance, *Bull. Seism. Soc. Am.* **61,** 231–240.

Ewing, W. M., W. S. Jardetzky, and F. Press (1957). *Elastic Waves in Layered Media,* McGraw-Hill, New York.

Gutenberg, B. (1945). Amplitudes of surface waves and magnitudes of shallow earthquakes, *Bull. Seism. Soc. Am.* **35,** 3–12.

Gutenberg, B. and C. F. Richter (1956). Magnitude and energy of earthquakes, *Ann. Geofisica.* **9,** 1–15.

Hanks, T. C. and H. Kanamori (1979). A moment magnitude scale, *J. Geophys. Res.* **84,** 2348–2350.

Herak, M. and D. Herak (1993). Distance dependence of M_s and calibrating function for 20 second Rayleigh waves, *Bull. Seism. Soc. Am.* **83,** 1881–1892.

Kanamori, H. (1978). Quantification of earthquakes, *Nature* **271,** 411–414.

Kaverina, A. N., A. V. Lander, and A. G. Prozorov (1996). Global creepex distribution and relation to earthquake-source geometry and tectonic origin, *Geophys. J. Int.* **125,** 125–265.

Lilwall, R. C. (1987). Station threshold bias in short-period amplitude distance and station terms used to compute body-wave magnitude m_b, *Geophys. J. R. Astr. Soc.* **91,** 1127–1133.

Marshall, P. D. and P. W. Basham (1972). Distribution between earthquakes and underground explosions employing an improved M_s scale, *Geophys. J. R. Astr. Soc.* **28,** 431–458.

Marshall, P. D. and E. W. Carpenter (1966). Estimates of Q for surface Rayleigh waves, *Geophys. J. R. Astr. Soc.* **10,** 549–550.

Nowroozi, A. A. (1986). On the linear relation between m_b and M_s for discrimination between explosions and earthquakes, *Geophys. J. R. Astr. Soc.* **86,** 687–699.

Nuttli, O. W. (1973). Seismic wave attenuation and magnitude relations of eastern North America, *J. Geophys. Res.* **78,** 876–885.

Okal, E. A. (1989). A theoretical discussion of time domain magnitude: the Prague formula for M_s and the mantle magnitude M_m, *J. Geophys. Res.* **94,** 4194–4204.

Panza, G. F., S. J. Duda, L. Cernobori, and M. Herak (1989). Gutenberg's surface-wave magnitude calibrating function: theoretical basis from synthetic seismograms, *Tectonophysics* **166,** 35–43.

Prozorov, A. and J. A. Hudson (1974). A study of the magnitude difference $M_s - m_b$ for earthquakes, *Geophys. J. R. Astr. Soc.* **39,** 551–564.

Richter, C. (1935). An instrumental earthquake magnitude scale, *Bull. Seism. Soc. Am.* **25,** 1–32.

Romanelli, F. and G. F. Panza (1995). Effect of source depth correction on the estimation of earthquake size, *Geophys. Res. Lett.* **22,** 1017–1019.

Scheidegger, A. E. (1985). Recent research on the physical aspects of earthquakes, *Earth. Sci. Rev.* **22,** 173–229.

Thomas, J. H., P. D. Marshall, and A. Douglas (1978). Rayleigh-wave amplitudes from earthquakes in the range 0–150°, *Geophys. J. R. Astr. Soc.* **53,** 191–200.

Vaněk, J., A. Zatopek, V. Karnik, N. V. Kondorskaya, Y. V. Riznichenko, E. F. Savarensky, S. L. Solov'ev, and N. V. Shebalin (1962). Standardization of magnitude scales, *Bull. Acad. Sci. USSR, Geophys. Ser.*, no. 2, 108–111 (English Translation).

von Seggern, D. H. (1970). Surface-wave amplitude versus distance relation in the western United States, SDL Report No. 249, Teledyne Geotech, Alexandria, Virginia.

von Seggern, D. H. (1977). Amplitude-distance relation for 20 second Rayleigh waves, *Bull. Seism. Soc. Am.* **67,** 405–411.

Wessel, P. and W. H. F. Smith (1995). New version of the Generic Mapping Tools released, *EOS* **76,** 329.

Department of Geology and Geophysics
University of Edinburgh
Grant Institute
West Mains Road
Edinburgh EH9 3JW, United Kingdom

Manuscript received 18 February 1997.